Atomic Spectroscopy

September/October 2006 Volume 27, No. 5

In This Issue:

ASPND7 27(5) 139–178 (2006)
ISSN 0195-5373

Issues also available electronically.

(see inside front cover)

Atomic Spectroscopy
Vol. 27(5) Sept./Oct. 2006

Printed in the United States and published six times a year by:

PerkinElmer Life and Analytical Sciences
710 Bridgeport Avenue
Shelton, CT 06484-4794 USA
http://www.perkinelmer.com

SUBSCRIPTION INFORMATION
Atomic Spectroscopy
P.O. Box 3674
Barrington, IL 60011 USA
Fax: +1 (847) 304-6865
E-mail: atsponline@yahoo.com

2006 Subscription Rates
- U.S. $60.00 includes third-class mail delivery worldwide; $20.00 extra for electronic file.
- U.S. $80.00 for airmail $20 extra for electronic file.
- U.S. $60.00 for electronic file only.
- Payment by check (drawn on U.S. bank in U.S. funds) made out to: "*Atomic Spectroscopy*"

Electronic File
Send request via e-mail to:
atsponline@yahoo.com

Back Issues/Claims
- Single back issues are available at $15.00 each.
- Subscriber claims for missing back issues will be honored at no charge within 90 days of issue mailing date.

Address Changes to:
Atomic Spectroscopy
P.O. Box 3674
Barrington, IL 60011 USA

Microfilm
Atomic Spectroscopy issues are available from:
University Microfilms International
300 N. Zeeb Road
Ann Arbor, MI 48106 USA
Tel: (800) 521-0600 (within the U.S.)
+1 (313) 761-4700 (internationally)

Guidelines for Authors

Atomic Spectroscopy serves as a medium for the dissemination of general information together with new applications and analytical data in atomic absorption spectrometry.

The pages of *Atomic Spectroscopy* are open to all workers in the field of atomic spectroscopy. There is no charge for publication of a manuscript.

The journal has around 1500 subscribers on a worldwide basis, and its success can be attributed to the excellent contributions of its authors as well as the technical guidance of its reviewers and the Technical Editors.

The original of the manuscript can be mailed to the editor in hard copy including electronic file on disk or CD (or simply by e-mail) in the following manner:

1. If mailed, provide text (double-spaced) and tables in hard copy plus on disk or CD with text and tables in .doc file; figures in doc or tif files.
3. Number the references in the order they are cited in the text.
5. Consult a current copy of *Atomic Spectroscopy* for format.
6. Editor's e-mail: anneliese.lust@perkinelmer.com

All manuscripts are sent to two reviewers. If there is disagreement, a third reviewer is consulted.

Minor changes in style are made in-house and submitted to the author for approval.

If a revision of the manuscript is required before publication can be considered, the paper is returned to the author(s) with the reviewers' comments.

In the interest of speed of publication, a pdf file of the typeset text is e-mailed to the corresponding author before publication for final approval.

Once the issue has been printed, each author receives a final pdf file of the article including 50 complimentary copies of the article and several copies of the complete issue.

Additional reprints can be purchased, but the request must be made before printing.

PerkinElmer. Inc., holds copyright to all material published in *Atomic Spectroscopy* unless otherwise noted on the first page of the article.

Anneliese Lust
Editor, *Atomic Spectroscopy*
PerkinElmer
Life and Analytical Sciences
710 Bridgeport Avenue
Shelton, CT 06484-4794 USA

Use of Sugar Cane Bagasse as Solid Phase Extractor for Cadmium Determination by FAAS

Elisangela Cardoso Lima Borges, *Adriana Paiva de Oliveira, Mercedes de Moraes, and José Anchieta Gomes Neto
Instituto de Química, Universidade Estadual Paulista, UNESP, 14801-970, P.O. Box 355, Araraquara, SP, Brazil

ABSTRACT

The present paper describes the use of sugar cane bagasse as solid phase extractor for cadmium determination after complexation of the analyte with ammonium diethyldithiophosphate (ADDP) and sorption of the Cd-DDP complexes on the solid support. The concomitants were separated using a flow injection analysis (FIA) system coupled to flame atomic absorption spectrometry (FAAS) for determination. The main parameters such as ADDP concentration, acid medium, flow rate, reaction coil length, and reaction time were investigated.

The results obtained with HNO_3 showed good accuracy and precision. The enhancement factor was 20.5 times for a 120-second preconcentration time, and the analytical frequency was 25 determinations per hour. The calibration curve was linear over the concentration range of 1–40 μg L^{-1} Cd with a LOD of 0.697 μg L^{-1} Cd and a relative standard deviation of 0.96% after 12 sucessive measurements of 30 μg L^{-1} Cd.

The proposed method was evaluated for the FIA-FAAS analysis of certified reference materials (tomato leaves, spinach leaves, and bovine liver) and Cd-spiked foods (shrimp, sardine, tuna, chicken liver and bovine liver). Good recoveries (80.0–97.1%) for the Cd-spiked samples and certified reference materials were obtained.

The results of bagasse-packed minicolumns were compared with Si-C_{18} packed minicolumns. The *F*-test was applied between Si-C_{18}/Bagasse minicolumns, Si-C_{18}/certified values, and bagasse/certified values. It was found that the results were in agreement with the certified values at a 95% confidence level.

INTRODUCTION

Sugar cane bagasse is a residue abundantly available from Brazilian industries that produce sugar and alcohol (1). It is a fibrous and low-density material with a wide range of particle sizes and high moisture content (2). Among the organic materials that have the capacity to adsorb metallic ion such as corncobs and peanut skin, sugar cane bagasse also has various other functional groups (carboxylates, carbonyls, phenolics, and aliphatic hydroxyls, etc.) that are responsible for the physical and chemical interactions with inorganic or organic species (3–5).

Removal of metallic ions from aqueous or organic solutions on solid supports has in recent years been studied (6). Several studies on the adsorption of metallic ions in sugar cane bagasse describe preparation methods for the activation of active sites: Extraction of a component from the pulp (cellulose, lignin, hemicellulose), pH control, and choice of suitable buffer (2,6–16). Separation and concentration of the metallic ion can be efficiently accomplished with the solid phase extraction (SPE) technique based on a powdered sugar cane bagasse-packed minicolumn.

*Corresponding author.
E-mail: : dri_poliv@ig.com.br
Fax: +55 16 3222-7932

Diethyldithiophosphates have been studied due to their ability to form very stable complexes with all sorts of metals even in a high acidic medium. In 1962, Bode and Arnswald (17) studied the potential of ammonium diethylditiophosphate (ADDP) in the acid medium extraction of Ag(I), As(III), Au(III), Bi(III), Cd(II), Cu(II), Hg(II), In, Mo, Ni, Os(IV), Pb(II), Pt(IV), Re(VII), Sb(III), Se(IV), Sn(V), Te(VI), and Tl(I). Alkaline metals, alkaline earth, and ferrous ions were not extracted. Therefore, besides achieving complexation in acid medium, the complexant allows separatation of the analytes from Na, K, Ca, Ba, and Fe. These elements are usually abundant in natural samples and foodstuffs, and may be considered interferents with AAS techniques (17).

The main objective of this paper was to study the use of natural sugar cane bagasse for cadmium determination. On-line complexation of the analyte was performed with ammonium diethylditiophosphate and sorption of the Cd-DDP complexes on a sugar cane bagasse-packed minicolumn. The sample was then analyzed using a flow injection (FIA) system and flame atomic absorption spectrometric (FAAS) detection.

EXPERIMENTAL

Instrumentation

A PerkinElmer® Model AAnalyst™ 100 flame atomic absorption spectrometer was used, equipped with a deuterium lamp background correction system (PerkinElmer Life and Analytical Sciences, Shelton, CT, USA). A PerkinElmer Lumina™ hollow cathode lamp (HCL) was used for the

determination of Cd at the analytical wavelength recommended by the manufacturer (λ=228.8 nm), with a lamp current of 4 mA, and a slit width of 0.7 nm. A time constant of 2 seconds was used for peak height evaluation. Cadmium was determined under optimium operating conditions with an oxidizing air/acetylene flame.

An Ismatec IPC-8 peristaltic pump (Cole-Parmer Instrument Co., Niles, IL, USA) was used with Tygon® or Viton® tubes for handling the solutions. An injector-commutador made of Perspex® (18) was manually operated to control both the preconcentration and the elution steps. A commercial column (Sep-Pak® Cartridges, Part No. 51910, Waters, Milford, MA, USA), filled with C_{18} immobilized on silica, with a particle size between 40 and 63 µm, was used for preconcentration/separation and to purify the ADDP solution. This same column model was used for the bagasse sorbent, replacing the original filling with approximately 700 mg of sugar cane bagasse.

A Multiwave® microwave oven sample preparation system, instead of quartz vessels, we used six 20-mL TFM pressure decomposition vessels since high temperatures were required. (Anton Paar, Graz, Austria), was employed for digestion of the samples.

Reagents, Solutions, and Samples

High purity water was obtained using Permution deionizer systems (resistivity 18.2 MΩ cm) (Permution System, Curitiba, PR, Brazil). All chemical reagents were of analytical grade: Nitric acid P.A., hydrochloric acid P.A., and hydrogen peroxide 29% (Merck, Darmstadt, Germany), and ethanol P.A. (Synth, Diadema, SP, Brazil). These acids were used throughout to prepare all solutions and as eluent in the flow injection system.

Reference solutions containing 0.5, 1.0, 10.0, 30.0, 40.0, 50.0, 500, 1500, and 2000 µg L^{-1} Cd were made by dilution from 1000 mg L^{-1} Cd stock solutions (Normex™, Carlo Erba, Milan, Italy) and prepared in 0.1% (v/v) HCl or HNO_3.

Ammonium diethyldithiophosphate (ADDP) (Aldrich, Milwaukee, WI, USA) was used for Cd complexation. A 4% (m/v) ADDP solution was prepared weekly by dissolution of 4 g ADDP in ≈ 20 mL of ethanol and dilution to 100–mL volume with deionized water. This solution was then purified in a Si-C_{18} packed minicolumn and stored in polyethylene flasks in the refrigerator.

Preparation of Minicolumn With Sugar Cane Bagasse

Sugar cane plants were purchased from a local sugar cane juicing plant in Araraquara, São Paulo State, Brazil. Ten sugar canes were thoroughly washed with water, peeled, and compressed to remove the sugar cane juice. The bagasse was washed with hot deionized water (70–90 °C) for 30 minutes and then dried at 50 °C for 24 h in a forced air oven. The dried bagasse was ground in a knive mill (RetschMühle, Retsch GmbH, Haan, Germany) and sifted through a 100-mesh screen.

The extraction preconcentration column was made using a 10.5-mm Sep-Pak column, packed with sugar cane bagasse. One of the ends was bored open to permit filling of the minicolumn. Dry sorbent (700 mg bagasse) was filled into the column and the end plugged with a piece of nylon. The column ends were sealed using short pieces of Tygon® tubing with appropriate inner and outer diameters (2-mm i.d) to form reliable connections with the injector rotor. The connection of the narrow end of the minicolumn to the injector rotor was made as short as possible in order to keep the dispersion to a minimum during elution, leaving the longer connection to the wider end of the minicolumn.

The proposed method was based on the solid phase extraction system described by Fernandes et al. (19) which determined Cd, Cu, and Pb in wine using solid phase extraction (minicolumn Si-C_{18}).

In the proposed method, a column with Si-C_{18} was perforated and the silica removed. The sugar cane bagasse was filled into the column and the end plugged with a piece of nylon. This microcolumn was compared to a new minicolumn Si-C_{18}.

Sample Preparation of Foods and Certified Standards

The sample sizes used for digestion were 500 mg of commercial foodstuff and 200–500 mg of the certified reference materials (see listings in Table I). All samples were dried at 100 °C and milled. Each sample was placed in a Teflon® digestion bomb, and 3 mL HNO_3, 2 mL H_2O, and 1 mL H_2O_2 were added, then capped, and placed in the outer PTFE vessel. The outer vessel was enclosed in a polypropylene jacket as a "security measure" which required the use of a wrench for fastening. Six bombs, including one blank, were positioned symmetrically on the carousel of the Multiwave microwave oven and heated simultaneously for 20 minutes. After the bomb reached room temperature, the caps of the bombs were removed and the digests diluted to 25 mL with deionized water. All samples were spiked with 10 mg L^{-1} Cd and three replicates were performed for each sample.

The microwave oven program used is summarized in Table II. The program for the digestion consisted of three temperature stages: The first stage allowed solubilization and preliminary digestion without

TABLE I
Analytical Results for Food Samples,
Recovery of Spiked Analytes and Certified Reference Materials (n=3)

Samples	Found (μg g^{-1})		Recovered (%) (Spiked: 10 μg g^{-1})	
	Si-C_{18}	Bagasse	Si-C_{18}	Bagasse
Shrimp	0.195±0.031	0.193±0.038	102±6.12	94.5±7.58
Tuna	0.169±0.016	0.163±0.015	96.3±3.27	89.2±3.03
Sardine	0.183±0.023	0.175±0.021	94.9±4.63	87.9±4.29
Bovine Liver	<0.754 μg g^{-1}	<0.697 μg g^{-1}	103±2.31	97.1±3.71
Chicken Liver	0.094±0.029	0.071±0.015	97.7±5.90	90.6±3.03

Certified Reference Material	Certified Value (μg g^{-1})	Found (μg g^{-1})	
		Si-C_{18}	Bagasse
Bovine Liver (NIST 1577b)	0.50±0.03	0.52±0.02	0.40±0.03
Tomato Leaves (NIST 1573a)	1.52±0.04	1.65±0.02	1.30±0.03
Spinach Leaves (NIST 1570a)	2.89±0.07	2.92±0.03	2.85±0.03

TABLE II
Microwave Program

Reagent Addition: 3.0 mL HNO_3 + 2.0 mL H_2O + 1.0 mL H_2O_2

Power (W)	Time (min)	Final Power (W)	Fan
100	5	500	1
800	15	800	1
0	15	0	3

excessive foaming; the second stage employed longer hold times and pressure to achieve a more efficient digestion; the final stage was used for cooling.

Flow Injection Analysis System

A flow injection analysis (FIA) system was developed to perform the separation and preconcentration of Cd^{2+} and the details of the optimized analytical performance for both columns filled with bagasse and Si-C_{18} are listed in Table III. In the preconcentration step depicted in Figure 1, sample S merges with the ADDP solution (reagent R) at the confluent point X. The Cd-DDP complexes formed in the reaction coil RC are retained by the bagasse or Si-C_{18} minicolumn MC. After a preset time, the injector commutador IC was switched to the alternative position in which the minicolumn was intercalated in the eluent line. In this situation, ethanol flows through the minicolumn, discharging the Cd-DDP complexes to the spectrometer. A transient absorbance was recorded with the peak height proportional to the analyte content in the sample. After peak measurement, the injector commutador was switched back to the initial position where another cycle can be started.

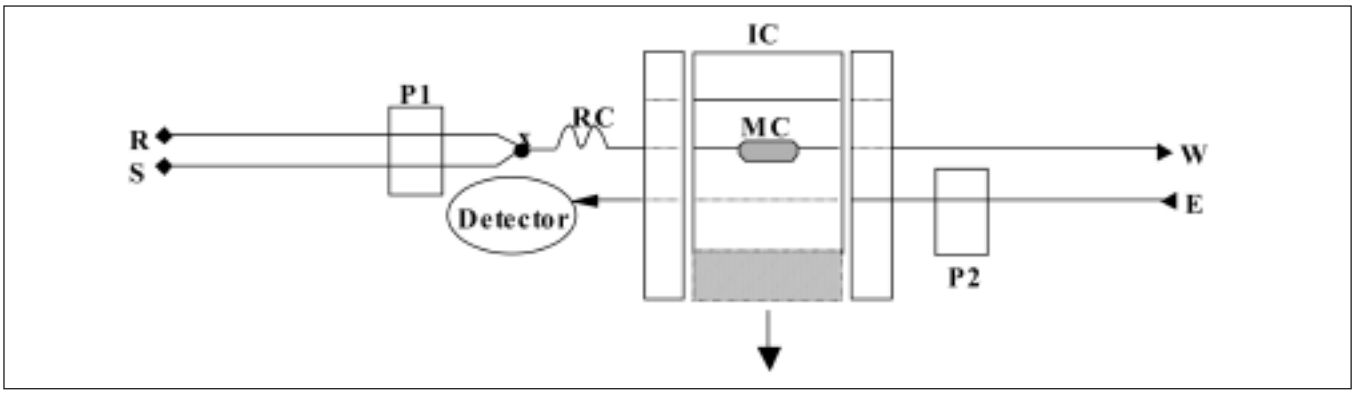

Fig. 1. FI manifold for on-line sorption preconcentration by FAAS. S: sample; R: chelating reagent; P1, P2: peristaltic pumps; X: confluence point; RC: reaction coil; IC: injector-commutador; MC: minicolumn; W: waste; E: eluent; detector: FAAS. The arrow down indicates the movement of the central part IC.

TABLE III
Analytical Performance of SPE-FIA-FAAS for Cd Determination

	HCl	HNO_3
ADDP Concentration (% m/v)	1.0	1.0
Length of Reaction Coil (cm)	10	10
Sample Flow Rate (mL min^{-1})	6.0	6.0
ADDP Flow Rate (mL min^{-1})	1.3	1.3
Ethanol Flow Rate (mL min^{-1})	6.0	6.0
Preconcentration Time (s)	120	120
	Bagasse	
Analytical Frequency (h^{-1})	26	25
Enhancement Factor	21.5	20.5
Direct Analytical Curve Range (μg L^{-1})	50–2000	50–2000
Preconcentration Analytical Curve Range (μg L^{-1})	10–40	1–40
Angular Coefficent (μg^{-1} L)	0.00301	0.00382
Linear Coefficient	0.00814	0.00599
Regression Coefficient	0.9996	0.9989
Characteristic Concentration (μg L^{-1})	1.45	1.14
Limit of Detection (μg L^{-1})	0.666	0.697
Limit of Quantification (μg L^{-1})	2.22	2.33
	Si-C_{18}	
Analytical Frequency (h^{-1})	25	24
Enhancement Factor	27	19
Direct Analytical Curve Range (μg L^{-1})	50–2000	50–2000
Preconcentration Analytical Curve Range (μg L^{-1})	1–40	1–50
Angular Coefficient (μg^{-1} L)	0.00379	0.00353
Linear Coefficient	0.00881	0.0002
Regression Coefficient	0.9915	0.9997
Characteristic Concentration (μg L^{-1})	1.15	1.24
Limit of Detection (μg L^{-1})	0.529	0.754
Limit of Quantification (μg L^{-1})	1.76	2.51

RESULTS AND DISCUSSION

The experimental parameters of the solid phase extraction-flow injection analysis-flame atomic absorption spectrometry (SPE-FIA-FAAS) system were optimized by using the univariate method; in other words, the values of all variables, except those of this study. Once a variable was optimized, it was maintained for use in subsequent studies. Optimization was accomplished after considering maximum absorbance signal, best repeatability, lowest relative standard deviation, and best transient signal profile.

Optimization of the SPE-FIA-FAAS system was accomplished by measuring the signals of a 100-μg L^{-1} Cd solution in 0.1% (v/v) HCl or HNO_3 with a preconcentration time of 120 seconds.

Configuration of Support

Different configurations of support were tested to pack the solid extractor: Syringes, tubes, micropipette tips, and sealed unit. Among the supports tested, the commercial cartrigde (Sep-Pak) provided best repeatability of measurements, transient peak profile, and lowest hydrodynamic pressure (observed as leakage at both ends of the column).

Concentration of Complexing Agent

The effect of ADDP was studied, keeping the flow rate at 0.7 mL min^{-1} for ADDP and at 3.0 mL min^{-1} for the sample solution. Ammonium diethyldithiophosphate was investigated in the 0.05–2.0% (m/v) range and at a preconcentration time of 30 seconds. This stage consisted of single measurements after sorption and elution of the analyte in the minicolumn with sugar cane bagasse. Minimum concentrations of ADDP were found for the quantitative extraction of cadmium in HNO_3 medium. For the HCl

medium, however, the signal intensities increased as a function of the ADDP concentration. A 1.0% (m/v) ADDP was used for the two acid mediums throughout this work.

Length of Reactor RC

After selection of the ADDP concentration, the influence of variation in the length of reactor RC was studied from 10–50 cm. In the HCl medium, the absorbance was constant for reactor lengths up to 20 cm; at higher lengths, the signals decreased by ~20% due probably to adsorption of Cd chlorides on the walls of the polyethylene tubing. For HNO_3, different RC lengths did not alter absorbance. Thus, the length of the reactor RC was fixed at 10 cm.

Sample Flow Rate

The effect of variation of sample loading flow rate on the collection of the metal-DDP chelate was also studied by changing the rotation speed of the peristaltic pump. The sample flow rate was studied in the 3.3–7.2 mL min^{-1} range. The absorbance increased with an increase in flow rates up to 6.0 mL min^{-1}, but the signals remained steady above that value. Therefore, this parameter was adjusted to 6.0 mL min^{-1} for use with HCl and HNO_3 in all further experiments. It should be noted that the flow rate of the ADDP was changed simultaneously with the sample in order to avoid variation in the ligand concentration. The flow rate of ADDP was fixed at 1.3 mL min^{-1} to avoid large dilutions of the analyte after the confluent point X and to guarantee minimum interaction time between analyte and ligand when forming the Cd-DDP complexes.

Eluent Flow Rate

When the ethanol flow rate was varied from 4.5–8.4 mL min^{-1}, HCl did not alter absorbance but precision was increased at a flow rate of 4.5 mL min^{-1}. On the other hand, in nitric medium, a 30% reduction in absorbance was observed when the ethanol flow rate was varied from 4.5–7.5 mL min^{-1}. Higher flow rates did not alter the signal. Even though high signals were obtained in the 4.5–5.5 mL min^{-1} range, best repeatability of measurements was obtained at the 6.0 mL min^{-1} flow rate. This flow rate was therefore selected for use with both HCl and HNO_3.

Preconcentration Time

The influence of variation of preconcentration time on sensitivity was studied in the 30–360 second range. For both acids (HCl and HNO_3), a linear correlation between absorbance and preconcentration time was found for the initial 180 seconds. A longer time can be used to improve the preconcentration factor or sensitivity. Therefore, a 120-second preconcentration time was used.

Acid Medium

It has been shown that both acids (HCl and HNO_3) provide good analytical results. However, nitric acid was chosen for the sample pretreatment procedure because it gave better sensitivity.

The developed FIA system for Cd determination was applied to food samples and certified reference materials (see Table III).

Analytical Features

The optimized parameters of the FIA system for Cd determination using columns packed with sugar cane bagasse and Si-C_{18} (19) are presented in Table III. Similar enrichment factors were obtained for both minicolumns. As also shown in Table III, there is no proportional difference between loading sample volume and enrichment factor for the studied sorbents. A simple explanation for this behavior cannot be provided. Retention-elution of the analyte is very much dependent on the characteristics of the sorbent material and certainly several factors contribute for the non-proportionality, such as partial elution of the analyte by sample volume, kinetics of sorption and elution reactions, saturation of active sites, etc.

Table III also lists the useful ranges of the analytical curves obtained using the optimized parameters and other analytical characteristics. The linearity of the curves (Figure 2) was acceptable considering the flame detector employed. It was observed that throughout about 100 preconcentration cycles, the sugar cane bagasse minicolumn did not present any extraction efficiency problems. After this, the column was re-filled with another 700-mg portion of bagasse. The Si-C_{18} packed column was used for more than 300 cycles and was still in good shape for more cycles.

The relative standard deviations (RSDs) were 0.74% (bagasse-HCl), 0.96% (bagasse–HNO_3), 0.96% (Si-C_{18}–HCl), and 0.99% (Si-C_{18}–HNO_3) after 12 sucessive measurements of 30 μg L^{-1} Cd. These results are adequate when considering, among other factors, that in the manual system used the columns could be packed in many ways for the different runs.

Applications

The proposed method was applied to the analysis of certified leaves (NIST 1573a and 1570a) and bovine liver (NIST 1577b) reference materials (National Institute of Standards and Technology, Gaithersburg, MD, USA). Also the following foods, obtained from local stores, were analyzed: Shrimp, tuna, sardines, bovine liver, and chicken liver (see Table I). Calibrations were performed using aqueous standard solutions. It can be seen that the recoveries of the certified materials and foods were satisfac-

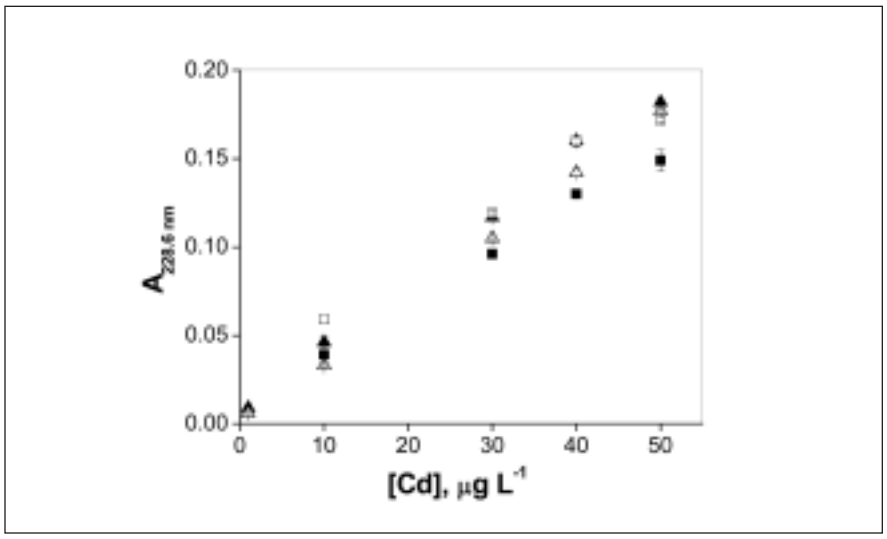

Fig. 2. Preconcentration analytical curve in sugar cane bagasse and Si-C_{18} minicolumns. Bagasse : ■ HCl, ▲ HNO_3; Si-C_{18}: □ HCl, Δ HNO_3; Acidity : 0.1% (v/v).

tory and resulted in a 95% confidence level.

The performance of the method with sugar cane bagasse used as sorbent was very good for all of the examined samples and equivalent to the results obtained with Si-C_{18}. The results show that the samples analyzed did not exceed the requirements of the Brazilian Food Regulations (20) for Cd concentrations (Decree #55871-ANVS from the Health Department, Brasília, Brazil). The maximum permissible level for fish was set at 1.0 μg g^{-1} Cd; however, no limits have yet been established for meats.
The *F*-test was applied to both Si-C_{18}/Bagasse minicolumns: Si-C_{18}/certified value and Bagasse/certified values.
The results were in good agreement with the certified values at a 95% confidence level.

CONCLUSION

The use of sugar cane bagasse-packed minicolumns is an advantageous alternative for Cd preconcentration and FAAS determination after complexation with ammonium diethyldithiophosphate. The application of sugar cane bagasse as a natural sorbent in systems of solid phase extration presented satisfactory results in terms of efficiency of extraction and comparable analytical resolution to the commercial Si-C_{18}.

The results obtained with HNO_3 showed good accuracy and precision. The enhancement factor was 20.5 times for a 120-second preconcentration time, and the analytical frequency was 25 determinations per hour. The calibration curve was linear over the concentration range of 1–40 μg L^{-1} Cd with a LOD of 0.697 μg L^{-1} Cd and a relative standard deviation of 0.96% after 12 sucessive measurements of 30 μg L^{-1} Cd. The minicolumn is effective, stable, and the results are reproducible. In addition, conditioning, activation, or washing steps are not necessary which increases analytical sample throughput.

ACKNOWLEDGMENTS

The authors are grateful to Fundação de Amparo à Pesquisa do Estado de São Paulo (FAPESP, Projects 99/10486-9 and 00/15118-7) for financially supporting this work and for a fellowship to E.C.B.L.

Received April 13, 2006.

REFERENCES

1. D.E. Teixeira, A.F. Costa, and M.A.E. Santana, Sci. Forens. 52 (1), 29 (1997).
2. M.G. Rasul, V. Rudolph, and M. Carsky, Fuel 78(1), 905 (1999).
3. N. Consolin Filho, A.A. Winkler-Hechenleitner, and E.A. Gómez-Pineda, Int. J. Polym. Mater. 34(1), 211 (1996).
4. J.M. Paiva and E. Frollini, J. Appl. Polym. Sci. 83(1), 880 (2002).
5. E.T.H. Costa, A.A. Winkler-Hechenleitner, and E.A. Gómez-Pineda, Sep. Sci. Technol. 30, 2593 (1995).
6. P.M. Padilha, J.T.S. Campos, J.C. Moreira, and C.C. Federici, Quim. Nova 18(6), 529 (1995).
7. W.S. Peternele, A.A. Winkler-Hechenleitner, and E.A. Gómez-Pineda, Bioresour. Technol. 68(1), 95 (1999).
8. A.N.A. El-Hendawy, S.E. Samra, and B.S. Girgis, Colloids Surf., A 180, 209 (2001).
9. P.M. Padilha, J.C. Rocha, J.C. Moreira, J.T.S. Campos, and C.C. Federici, Talanta 45, 317 (1997).
10. M. Rao, A.V. Parwate, and A.G. Bhole, Waste Managemt. 22(1), 821 (2002).
11. W.E. Marshall, D.E. Waterlle, D.E. Boler, M.M. Johns, and C.A. Toles, Bioresour. Technol. 69, 263 (1999).
12. M.C. Basso, E.G. Cerrella, and A.L. Cukierman, Ind. Eng. Chem. Res. 41, 3580 (2002).
13. K.A. Krishnan and T.S. Anirudhan, Ind. Eng. Chem. Res. 41, 5085 (2002).

14. D. Mohan and K.P. Singh, Water Res. 36, 2304 (2002).

15. C.J. Lin and J.E. Chang, Chemosphere 42, 1185 (2001).

16. G. Vásquez, J. González-Álvarez, S. Freire, M. López-Lorenzo, and G. Antorrena, Bioresour. Technol. 82, 247 (2002).

17. H. Bode and W. Arnswald, Fresenius Z. Anal. Chem. 185, 179 (1962).

18. F.J. Krug, H. Bergamin Filho, and E.A.G. Zagatto, Anal. Chim. Acta.179, 103 (1986).

19. A.P. Fernandes, M. Moraes, and J.A. Gomes Neto, At. Spectrosc. 24(5), 179 (2003).

20. http://www.anvisa.gov.br/alimentos/legis/especifica/contaminantes

Electrothermal Atomic Absorption Spectrometry: A Method for Characterizing Atomization Profiles

***A.R. Maurí-Aucejo, A. Campos-Candel, and M. Llobat-Estellés**
Department of Analytical Chemistry. University of Valencia
Dr. Moliner 50, E-46100 Burjassot, Valencia, Spain

ABSTRACT

A method is proposed to characterize the shape of the atomization profiles of standard solutions and samples obtained by electrothermal atomic absorption spectrometry. Changes in the shape of these profiles indicate the existence of matrix influences and permit the detection of possible sources of bias errors due to the use of an inadequate standard. The proposed procedure was applied to atomization profiles of copper in the presence of NaCl and to atomization profiles of chromium in oil samples after two alternative sample pretreatments. The results indicate that the proposed model is capable of detecting changes in the copper atomization profiles in the presence of 0.15% of NaCl. On the other hand, the study of chromium atomization profiles indicates that after acid treatment it is possible to use aqueous standards because no differences were found between the two atomization profiles. However, after basic treatment, different atomization profiles were obtained which eliminates the use of aqueous standards. The proposed procedure is a useful tool to check if the standard employed is suitable to obtain accurate results, specifically for the determination of metallic elements in samples with a complex matrix that is not completely destroyed after the sample pre-treatment step.

INTRODUCTION

The determination of metallic elements by electrothermal atomic absorption spectrometry (ETAAS) is based on the vaporization of the sample, and the subsequent generation of atomic vapors using a graphite furnace. This atomic vapor produces a transitory signal A=f(t) proportional to the concentration of the analyte in the sample. ETAAS constitutes an essential tool for the determination of metals at trace levels due to its high selectivity and sensitivity. However, there are several sources of error whose origins are found, in most cases, in the nature of the matrix of the sample and, therefore, elimination of these errors is of great importance. The nature of the sample also affects the process of atomization of the analyte. Moreover, if the matrix cannot be eliminated in the mineralization step, it can introduce serious spectral interferences since non-specific absorptions or overlap atomic peaks less frequently, although these can be increased if Zeeman background correction is used (1). None of the various proposed solutions has managed to definitely solve the problem of the matrix and the subject remains of interest (2).

Atomization of the analyte, that is to say, the formation of atomic vapor depends on diverse chemical and physical factors that have been thoroughly studied (3). To obtain an exact result, it is essential that the transitory signals A=f(t) (atomization profiles) are identical for both the standards and the samples.

**Corresponding author.*
E-mail: adela.mauri@uv.es

Characterizing the atomization profiles is therefore a prerequisite for an adequate analytical procedure. Such characterization can be achieved through several procedures described in the bibliography. For instance, L'vov has used a series to time values which effectively characterize atomization profiles (4,5).Barnett and Cooksey (6) describe a procedure to calculate the appearance time of the peak (t_{app}), the maximum absorbance time (t_{peak}), the end time (t_{end}), the atomization time (τ_1), and the mean residence time of the atoms in the furnace (τ_2) (Figure 1). Harnly increases the number of critical parameters by considering the time at which the signal of absorbance decays to half its value ($t_{1/2}$) (7). Wegscheider et al. (8) use eight descriptors as the critical parameters to detect changes in the sensitivity between standards and samples (peak area to peak height ratio, the mean and mode of the absorbance signal, the standard deviation, skewness and kurtosis of the free atom distribution, the baseline noise, and the appearance time of the peak). Sadler et al. (9) use the wavelet transforms to produce a number of quantitative measures of the signal variation, called Lipschtiz regularities, whose values depend on the shape of the atomization profile.

The present work proposes a method for the characterization of atomization profiles which is mathematically simpler than the model proposed by Sadler et al. On the other hand, in comparison to methods based on time parameters, the characterization of atomization profiles can be most reliable because the proposed method uses all absorbance values between t_{app} and t_{end}.

The proposed method is applied to profiles of Cu obtained in the presence of a synthetic matrix (different amounts of NaCl) and to profiles of Cr in a real matrix sample,

Atomic Spectroscopy
Vol. 27(5), Sept./Oct. 2006

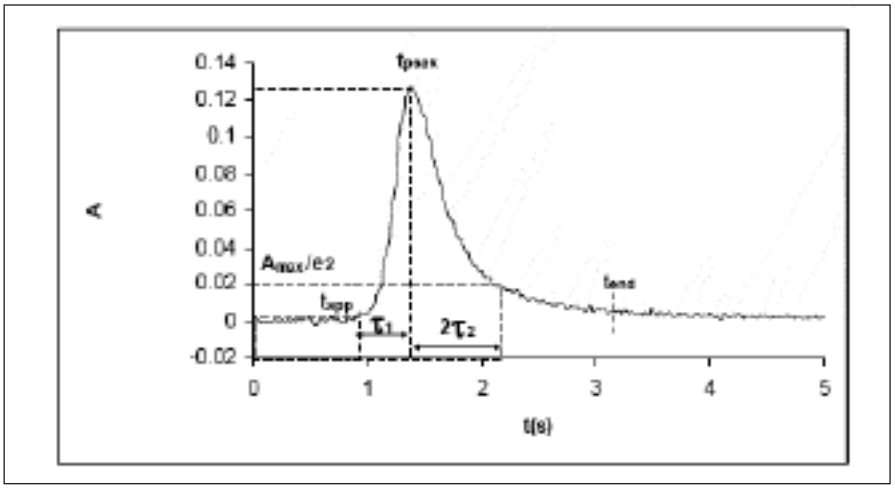

Fig. 1. Time parameters of peak profiles proposed by Barnett and Cooksey (6).

such as edible oil. Metals in oils are present in an organometallic form and for their determination in an aqueous standard require a sample pre-treatment step. In our study, two different sample treatments as described in the bibliography were used: an acid and a basic treatment (10–12). Moreover, the characterization of the atomization profiles is carried out using the procedure proposed by Barnett and Cooksey (6). The results show that our method improves the quality of the analytical data produced by ETAAS.

THEORETICAL

Characterization of the Atomization Profiles

Characterization curves are obtained by plotting $F_{t_i} = f(t_i)$, where F_{t_i} is the ratio between the absorbance value of the analyte in the sample at t_i and the absorbance value of the analyte in a solution considered as the contrast solution:

$$F_{t_i} = \frac{(A^s)_{t_i}}{(A^c)_{t_i}} \qquad \text{Eq. 1}$$

where $(A^s)_{t_i}$ and $(A^c)_{t_i}$ are the absorbance values at each time t_i from the atomization profile of the analyte in the sample and in the contrast solution, respectively.

There are two alternatives for the selection of contrast solutions: either a solution containing only the analyte or a solution containing the sample and added analyte (spiked sample). If the characterization curves are obtained using a spiked sample as the contrast solution, F_{t_i} is calculated as:

$$F_{t_i} = \frac{(A^s)_{t_i}}{(A^{S+P})_{t_i}} \qquad \text{Eq. 2}$$

where $(A^s)_{t_i}$ and $(A^{S+P})_{t_i}$ are the absorbance values at each time t_i for the atomization profile of the analyte in the sample and the spiked sample, respectively. If it is considered that:

$$(A^s)_{t_i} = C^S_A(f^S_A)_{t_i} \qquad \text{Eq. 3}$$

$$(A^{S+P})_{t_i} = C^S_A(f^S_A)_{t_i} + C^P_A(f^P_A)_{t_i} \qquad \text{Eq. 4}$$

where (f^S_A) and (f^P_A) are the response factors of the analyte at each time in the sample and the standard, and C^S_A and C^P_A are their respective concentrations, the F_{t_i} values can be expressed as:

$$(F)_{t_i} = \frac{C^S_A(f^S_A)_{t_i}}{C^S_A(f^S_A)_{t_i} + C^P_A(f^P_A)_{t_i}} \qquad \text{Eq. 5}$$

Then, if the atomization profiles of the analyte in the sample and the standard are identical or proportional from the appearance time of the peak (t_{app}) to the end time of the peak (t_{end}), the values can be expressed as:

$$(f^S_A)_{t_{app}} = k(f^P_A)_{t_{app}}$$
$$\ldots\ldots\ldots\ldots\ldots\ldots\ldots\ldots \qquad \text{Eq. 6}$$
$$\ldots\ldots\ldots\ldots\ldots\ldots\ldots\ldots$$
$$\ldots\ldots\ldots\ldots\ldots\ldots\ldots\ldots$$
$$(f^S_A)_{t_{end}} = k(f^P_A)_{t_{end}}$$

Equation 5 can be simplified as:

$$(F)_{t_i} = \frac{kC^S_A}{kC^S_A + C^P_A} \text{ CONSTANT} \qquad \text{Eq. 7}$$

On the other hand, if the characterization curves are obtained considering an analyte solution as the contrast solution, the same conclusions are obtained. In this case, F_{t_i} is defined as the ratio between $(A^S)_{t_i}$ and $(A^P)_{t_i}$, where:

$$(A^P)_{t_i} = C^P_A(f^P_A)_{t_i} \qquad \text{Eq. 8}$$

Then, Equation 7 can be simplified as:

$$(F)_{t_i} = \frac{C^S_A}{C^P_A} \text{ CONSTANT} \qquad \text{Eq. 9}$$

Meaning, F_{t_i} will acquire a constant value independent of t_i for which $F_{t_i} = f(t_i)$ will be a straight line of zero slope and intercept depending on the ratio of the concentrations. However, if:

$$(f^S_A)_{t_i} \neq (f^P_A)_{t_i}$$

the value of F_{t_i} will not be constant and $F_{t_i} = f(t_i)$ will not be a straight line with a zero slope, then the atomization profiles of the analyte in the sample and in the contrast solution are different.

When the atomization profiles of the analyte in the sample and in the contrast solution are different, the characterization curves can present many variable forms similar to the Apparent Content Curves Method proposed by Llobat et al. (13) to

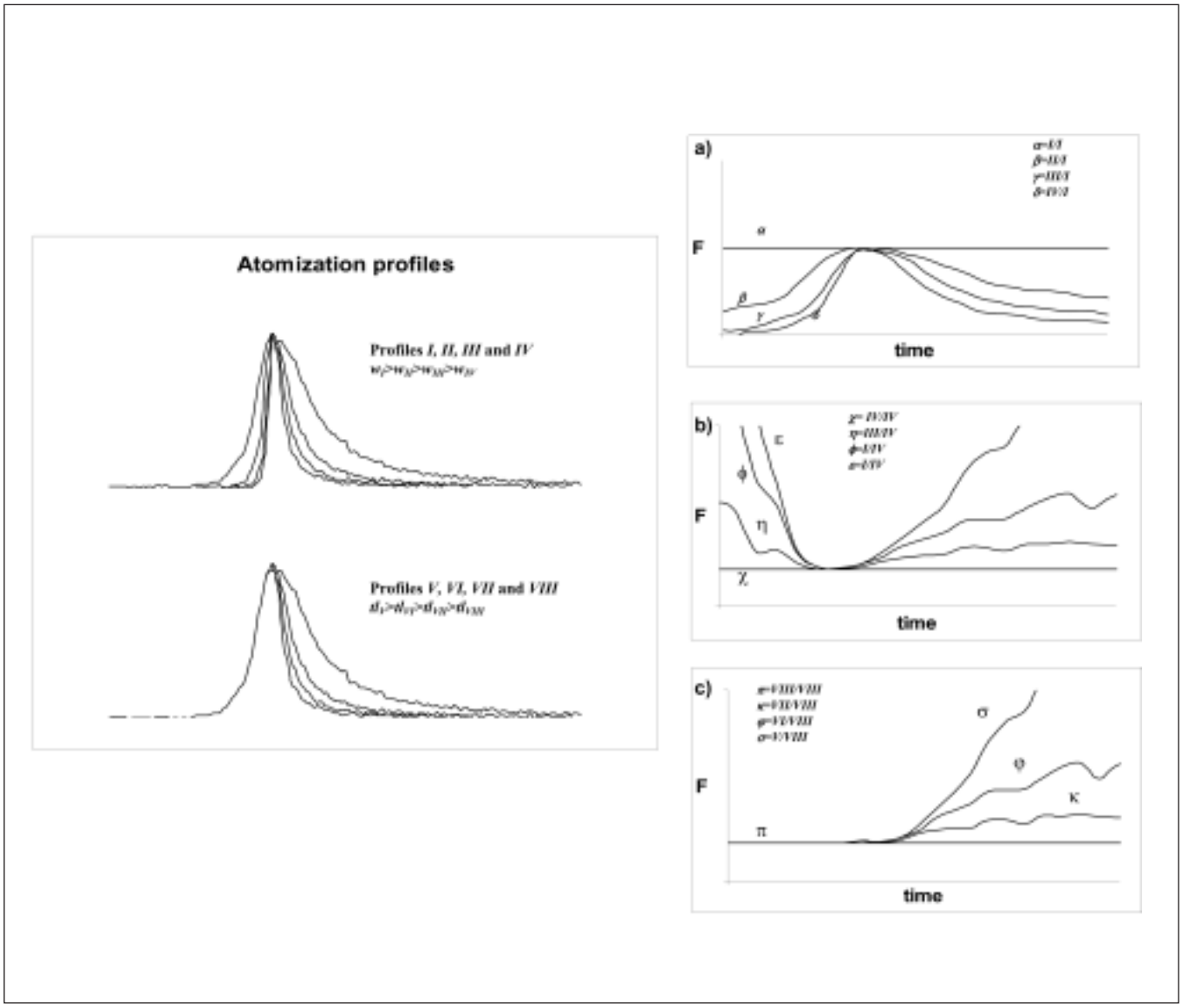

Fig. 2. Characterization curves obtained from peak profiles with coincident t_{peak}. (a) and (b) from peak profiles with several widths, (c) from several tailing peaks (tl).

evaluate spectral interferences in molecular spectroscopy. Figures 2 and 3 show the appearance of the characterization curves obtained from atomization profiles of the analyte and the contrast with different widths and/or t_{peak}:

• If t_{peak} coincides for both atomization profiles (analyte in the sample and analyte in the contrast solution), the curvature of the characterization curves is a function of the relation between the atomization profile widths. Therefore, when the difference in the atomization profile widths increases, the curvature increases and the characterization curves clearly differ from a straight line (Figure 2).

• If t_{peak} does not coincide for both atomization profiles, the obtained shape of the curves is varied, depending on both the width and the difference between t_{peak} of the analyte and the contrast solution (Figure 3).

Pattern Curve

As has been indicated above, the characterization curves obtained for identical atomization profiles must be straight lines with zero slopes. To obtain these curves it is necessary, firstly, to establish the time the profile appears and the final time and, once obtained, to estimate the reproducibility of the same by calculating the confidence bands.

Atomic Spectroscopy
Vol. 27(5), Sept./Oct. 2006

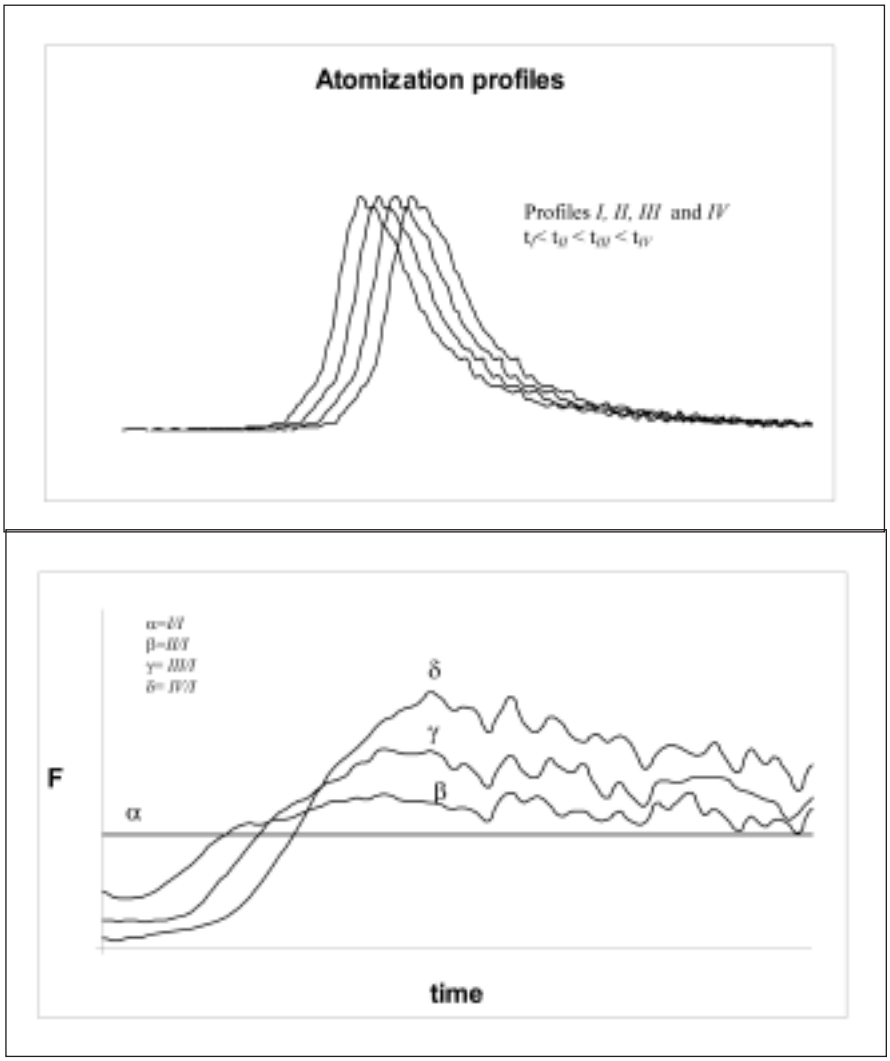

Fig. 3. Characterization curves obtained from peak profiles without coincident t_{peak}.

Therefore, the proposed model begins by recording the atomization profiles of (n+1) aqueous standards and the calculation of both, as well as the time the peak appears (t_{app}) and the time when the transitory signal disappears (t_{end}). Several procedures (6,7) are described in the bibliography to determine the t_{app} and the t_{end}, the use of derivative signals, and the use of the standard deviation. In the present work, the procedure described by Harnly (7) is applied for the determination of the time interval and t_{app} is considered as the one corresponding to an absorbance signal equal to four times the deviation of a blank (s_{Blank}). Similarly, the final time corresponds to the same absorbance value after the peak. A deviation of the baseline is obtained from background noise, being the maximum signal variation at times far from the peak corresponding to $5s_{Blank}$.

Once the time interval has been worked out, the different characterization curves are obtained and, from them, a pattern curve with its corresponding confidence bands is established as follows.

• Considering as contrast one of the obtained profiles, *n* characterization curves are obtained and, then, *n* normalized characterization curves are obtained from the normalized values of F_{t_i} (F_t^N):

$$(F_{t_i}^N) = \frac{F_{t_i}}{\overline{F}} \qquad \text{Eq. 10}$$

where:

$$\overline{F} = \frac{1}{n} \sum_{t_i = t_{app}}^{t_i = t_{end}} F_{t_i} \qquad \text{Eq. 11}$$

Finally, for each time the standard deviation is obtained from all normalized characterization curves, and the confidence band established as $F_{t_i}^{mean} \pm s_{t_i}$, where $F_{t_i}^{mean}$ is the average of $F_{t_i}^N$ for all curves at each t_i. From these values the Pattern Curve is plotted as $F_{t_i}^{mean} \pm s_{t_i}$ vs. t_i.

Characterization Curve of Analyte in the Sample

The characterization curve of the analyte in the sample is obtained by plotting $(A^S)_{t_i} / (A^C)_{t_i}$ vs. t_i for the different replicates of the sample and by establishing their confidence level analogous to the pattern curve. From this, the $F_{t_i}^{mean} \pm s_{t_i}$ vs. t_i curve is obtained. The terminology/symbols used for the equations are listed in Figure 4.

In this way, if the confidence bands of the characterization curve of the sample under study overlap with the confidence bands of the pattern curve, it can be concluded that the atomization profiles of both, contrast solution and sample, are not significantly different.

Matrix Under Study

For the application of the proposed procedure, two systems were chosen.

(a) One of the systems is the atomization profiles of copper in the presence of NaCl. This system was studied by Sadler et al. (14)

F_{i_j} the ratio between $(A^S)_{i_j}$ and $(A^C)_{i_j}$ at t_i

$(A^C)_{i_j}$ absorbance values at each time t_i for the atomization profile of analyte in the contrast solution

$(A^S)_{i_j}$ absorbance values at each time t_i for the atomization profile of analyte in the sample

$(A^{S+A^*})_{i_j}$ absorbance values at each time t_i for the atomization profile of analyte in the spiked sample

$(A^*)_{i_j}$ absorbance values at each time t_i for the atomization profile of analyte in a standard solution

$(f_A^S)_{i_j}$ the response factor of the analyte at each t_i in sample

$(f_A^{S^*})_{i_j}$ the response factor of the added analyte at each t_i in the spiked sample (or standard solution)

c_A^S the concentration of the analyte in sample

$c_A^{S^*}$ the concentration of the analyte added in spiked sample

$(F_{i_j}^N)$ normalized values of F_{i_j} calculated as the ratio between F_{i_j} and $\overline{F}$

$\overline{F}$ mean value of F_{i_j} from t_{app} to t_{end}

$F_{i_j}^{mean}$ the average of $F_{i_j}^N$ at each t_i from replicates of Characterization Curves

s_{i_j} the standard deviation of $F_{i_j}^N$ at each t_i from replicates of Characterization Curves

The time of critical peak parameters:

t_{app} the appearance of peak

t_{peak} the peak maximum

t_{end} the peak end of the atomization profile

τ_1 the atomization time of the atomization profile

τ_2 the mean residence time of atoms in the furnace

t_{1/e^2} the time for the signal to decline to $1/e^2$ of the maximum

Fig. 4. Terminology/symbols as used for equations.

who applied the wavelet transforms to produce a number of quantitative measures of the signal variation, called Lipschtiz regularities, and whose values depend on the shape of the absorbance profile. The results obtained by Sadler indicate that variations of the atomization profiles of copper exist in the presence of small amounts of NaCl.

(b) The other system chosen was the atomization profiles of chromium. Heavy metals have a negative influence on the oxidative stability of edible oils and fats. Their determination is usually carried out by atomic spectroscopy after pre-treatment of the sample. Several procedures were developed; the most common is the use of an organic solvent, ashing, acid digestion, or treatment with KOH in alcohol (10–12). On the other hand, if aqueous solutions are obtained after sample pre-treatment, calibration is carried out by aqueous stock solutions. Moreover, the standard addition method is generally used to avoid matrix effects.

EXPERIMENTAL

Instrumentation

All data were obtained using a PerkinElmer® Model 4100 ZL atomic absorption spectrometer (PerkinElmer Life and Analytical Sciences, Shelton, CT, USA). For all experiments, a PerkinElmer THGA™ transversely heated graphite furnace atomizer with graphite tubes was used. The temperature program and the experimental conditions utilized are summarized in Table I.

A microwave oven Model Samsung M182DN was also used for sample treatment (Telford, UK).

Standard Solutions and Reagents

A stock solution of copper (1000 mg/L) was prepared from 1 g of copper metal in 50 mL of 5M nitric acid and diluted to 1 L with NANOpure® Diamond™ Model D11941 water (Baernstead, Dubuque, IA, USA).

A stock solution of chromium (1000 mg/L) was prepared from 1 g of chromium metal in 50 mL of hydrochloric acid and 2 mL of nitric acid, and diluted to 1 L with NANOpure water.

Nitric acid utilized was Suprapur® (Merck, Darmstadt, Germany).

Chromium standard dissolved in oil of 1 g/kg CertiPUR® (Merck).

All other reagents used were of analytical grade.

Sample Pre-treatment

For the characterization of the atomic profiles of chromium in oil, a chromium standard in oil was used as the sample and an aqueous stock solution was used to obtain the spiked samples (by addition of 10 µg/L of Cr). Two treatments were chosen for the treatment of oil:

Atomic Spectroscopy
Vol. 27(5), Sept./Oct. 2006

TABLE I
Experimental Conditions

Step	Copper			Chromium		
	Temp. (°C)	Ramp Time (s)	Time (s)	Temp. (°C)	Ramp Time (s)	Time (s)
Dry Temperature	110	1	10	100	1	30
	130	5	15	140	15	30
Pyrolysis Temperature	750	10	5	1500	10	20
	800	10	4			
Atomization Temperature	2100	0	5	2300	0	5
Cleaning Temperature	2450	1	5	2450	1	3
Background Correction	Zeeman			Zeeman		
Matrix Modifier	10 µL of HNO_3 0.2%			None		
Injection Volume of Sample	10 µL			10 µL		

(a) Basic Treatment:

The sample (1–2 g) was placed in a 10-mL borosilicate glass and Teflon®-faced neoprene septa. Then, 4 mL of an ethanolic solution of KOH 3M was added and, after shaking for about 1 minute, water was added and the solution shaken again. The resulting solution was left standing until completely clear. Finally, the solution was diluted with Nanopure water to 10-mL volume. The spiked samples were prepared by addition of an aliquot of the chromium stock solution before the dilution step.

(b) Acid Treatment:

The samples (1–2 g) and 6 mL of HNO_3 (1:1) were placed in Teflon vessels. The vessels were placed into a commercial type microwave oven and heated in four steps by using medium power for 2 min, 1 min, 1 min, and 1 min, respectively, and cooling between steps. After acid digestion, the solution was placed into a vessel and diluted to 10-mL volume. The spiked samples were prepared by addition of an aliquot of the chromium stock solution before the dilution step.

RESULTS AND DISCUSSION

Characterization of Atomization Profiles of Copper in Presence of NaCl

The pattern curve corresponding to the atomization of Cu, using the instrumental conditions previously indicated, was obtained as follows:

First, aqueous solutions containing different amounts of copper were prepared and their atomization profiles registered. Next, the time interval of the profiles was established by calculating the time at which the peak appears (t_{app}) and the time when the transitory signal disappears (t_{end}). Then, taking one of the profiles as a reference, the values of F_{t_i} were calculated, and the normalized values for each characterization curve obtained. Finally, its corresponding standard deviations were also calculated.

Figure 5 shows the pattern curve obtained. As can be seen, the experimental pattern curve logically differs from the theoretical pattern curve (straight line of zero slope) because it is obtained from experimental points. On the other hand, the standard variation is greater at times near t_{app} and t_{end} because the absorbance values are lower than the absorbance values at times near t_{peak} and, therefore, more non-reproducible.

To obtain the characterization curves of atomization profiles of copper in the presence of NaCl, solutions containing different amounts of NaCl (0.006%, 0.05%, 0.15%, 0.7%, 1%, 2%, and 5%) and a fixed amount of Cu (80 g/L) were prepared and their profiles registered. Next, considering as contrast a solution without NaCl, the characterization curves were obtained. Finally, the values of F_{t_i} were normalized, the confidence band calculated, and the curves thus obtained placed on the pattern curve from the standards (Figure 6).

As can be seen, when the amount of NaCl increases, the characterization curves are out of the confidence band of the pattern curve, being clearly different from 0.15% of NaCl.

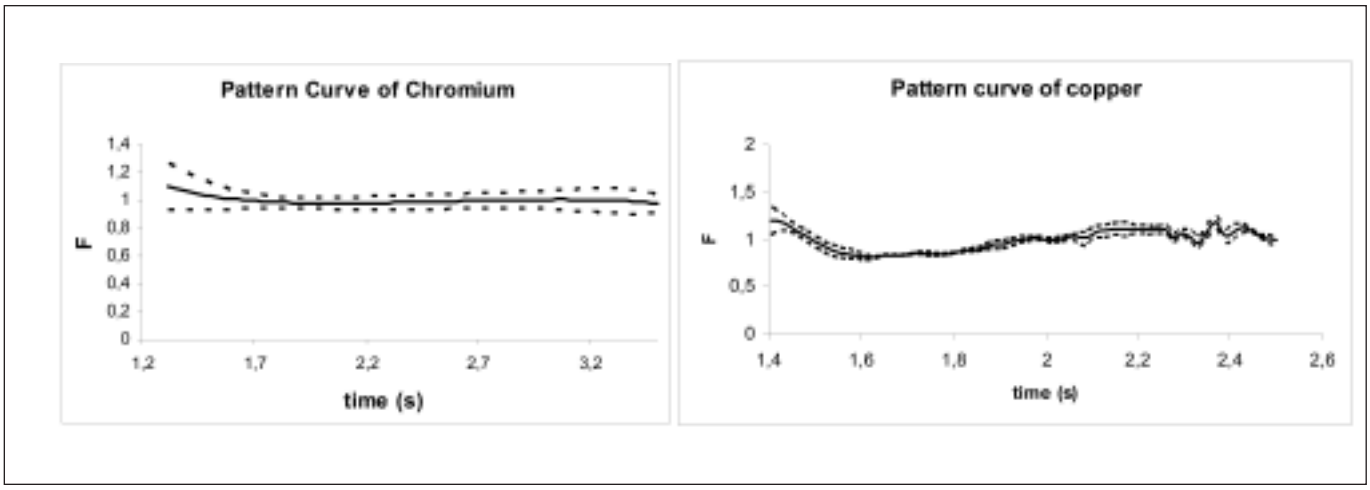

Fig. 5. Pattern curves obtained from aqueous standard solutions of copper and chromium.

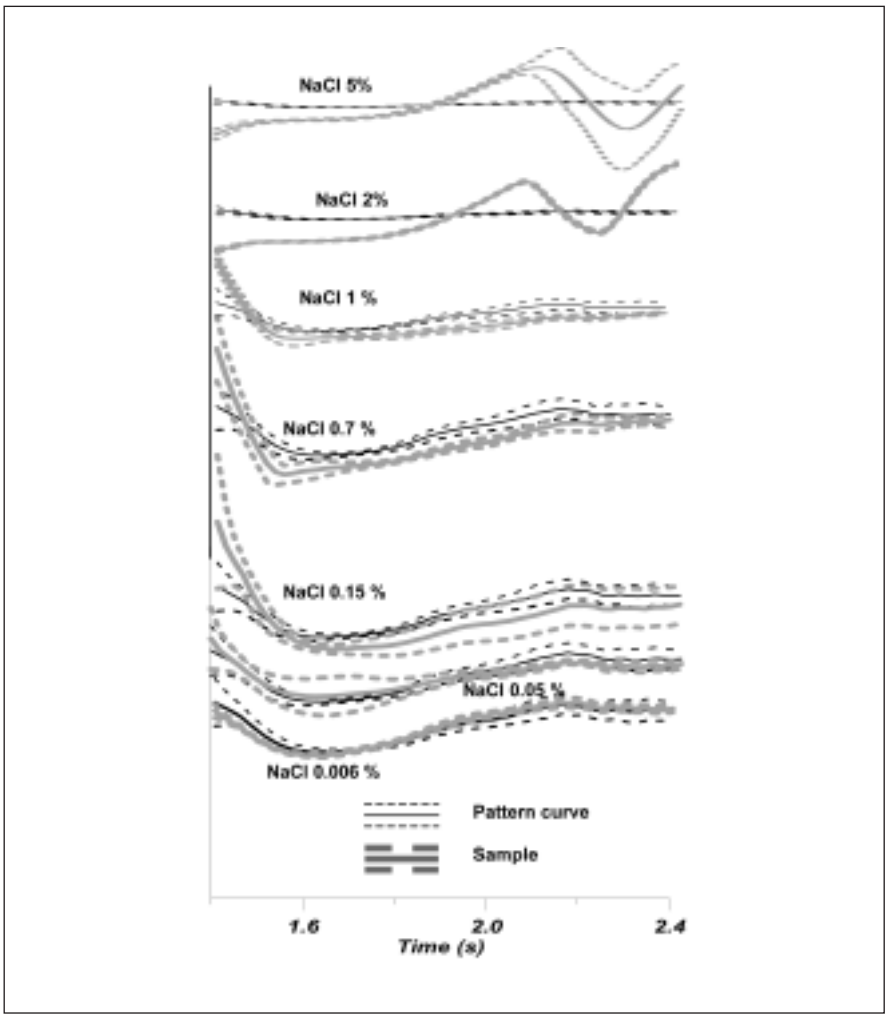

Fig. 6. Characterization curves obtained for solutions of copper containing different amounts of NaCl.

Characterization Atomization Profiles of Copper in Presence of NaCl by Barnett and Cooksey Method

Following the procedure proposed by Barnett and Cooksey (6), the peak parameters, which describe the atomization profiles, were calculated as follows:

• The appearance of peak (t_{app}) as the value of time, which causes the first derivative to become positive.

• The peak maximum (t_{peak}) as the value of time, which causes the first derivative to equal zero.

• The peak end (t_{end}) can be calculated as the value of time, which causes the first derivative to return to zero. However, the absorbance signal returns exponentially to baseline and it is difficult determine the time at which the first derivative returns to zero. Then, the end time is calculated as $\tau_1+4\tau_2$ (suggested as the minimum integration time by L'vov):

• The atomization time (τ_1) as $t_{peak}-t_{app}$

• The mean residence time of atoms in the furnace (τ_2) as

$$\frac{(t_{1/e^2} - t_{peak})}{2}$$

where $t_{1/e}^2$ is the time for the signal to decline to $1/e^2$ of maximum.

The values of these parameters were obtained for different solutions without NaCl and the confidence band of each parameter calculated. On the other hand, the values of time parameters for solutions containing different amounts of NaCl were calculated following the same procedure. Table II shows the confidence bands obtained for each time parameter in the absence of NaCl (reference value) and the values of the peak parameters from the atomization profiles of the analyte in the presence of each concentration of NaCl. For solutions containing 2% and 5% of NaCl, it is not possible to calculate these parameters because of the noise of the derivative atomization profiles.

From the results obtained, it can be concluded that there is a deviation of the peak parameters due to NaCl, but these deviations are low and do not have any relation to the amount of NaCl. For instance, the t_{app} value for the solution containing 0.05% of NaCl is out of the reference value, but the t_{app} value for the solution containing 0.7% of NaCl coincides with the reference value. The same contradiction is observed in the τ_1 value for the solution containing 1% of NaCl, which is coincident with the reference value. Finally, for each tested solution the five peak parameters gave us contradictory information. As indicated by Salder et al. (14), the performance of the time parameter procedure is inadequate for detecting small changes in the atomization profiles.

Characterization of Atomization Profiles of Chromium in Oil

Figure 5 shows the pattern curve corresponding to the atomization of Cr, obtained under the instrumental conditions previously indicated, and following the same procedure as for the pattern curve of Cu.

The atomization profiles of chromium in the oil samples and the spiked samples were obtained and, with the spiked samples used as the contrast samples, the characterization curves and their confidence bands were obtained as described above. Finally, they were placed on the pattern curve obtained from the standards (Figure 7).

As can be seen, the characterization curves obtained after the basic treatment are out of the confidence band of values obtained for the pattern curve. However, the characterization curves obtained after acid digestion coincide with the confidence band of values obtained for the pattern curve.

Following the procedure proposed by Barnett and Cooksey (6), the peak parameters were calculated from the atomization profiles of chromium in oil after basic and acid treatment and for their respective spiked samples. The results are listed in Table II.

TABLE II
Peak Parameters Obtained From Atomization Profiles of Copper and Chromium

Sample	t_{app} (s)	t_{peak} (s)	t_{end} (s)	τ_1(s)	τ_2 (s)
Copper in Presence of NaCl					
0% of NaCl (Reference value)	1.02±0.05	1.64±0.02	2.87±0.05	0.62±0.03	0.56±0.04
0.006% of NaCl	1.05	1.64	2.91	0.59	0.58
0.05% of NaCl	1.24[a]	1.64	2.70[a]	0.42[a]	0.57
0.15% of NaCl	1.12[a]	1.66	2.94[a]	0.54[a]	0.60
0.7% of NaCl	1.06	1.62	3.11[a]	0.55[a]	0.64[a]
1% of NaCl	1.09[a]	1.71[a]	2.98[a]	0.62	0.59
Chromium in Oil					
Oil - Basic Treatment (Reference Value)	0.88±0.03	1.476±0.011	2.15±0.03	0.60±0.02	0.388±0.006
Spiked Oil - Basic Treatment	0.97[a]	1.48	2.07[a]	0.51[a]	0.39
Oil - Acid Treatment (Reference value)	0.53±0.06	1.303±0.011	3.93±0.17	0.77±0.05	0.79±0.04
Spiked Oil - Acid Treatment	0.54	1.31	3.78	0.74	0.76

[a]Out of the reference value.

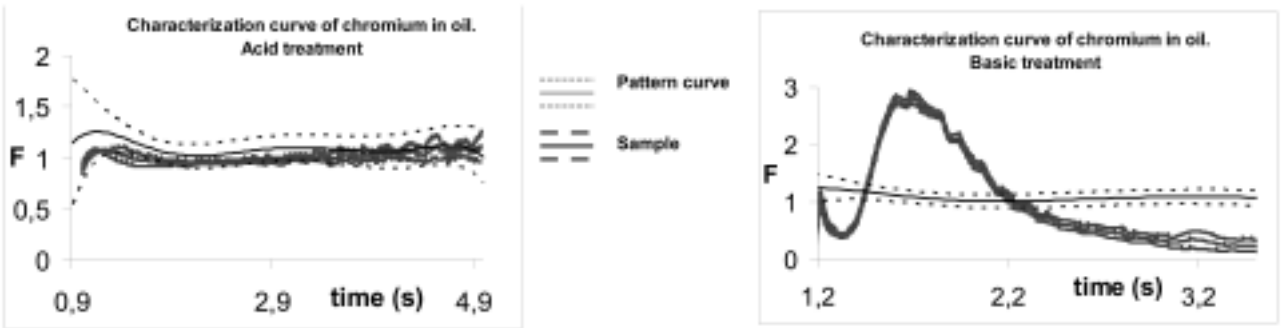

Fig. 7. Characterization curves obtained for chromium in oil after basic and acid treatment.

As can be seen, the values obtained are not significantly different for sample and spiked sample after acid treatment. However, after basic treatment, the time of the critical peak parameters of the sample and spiked sample differs although, similar to the copper-NaCl system, the differences are minimal.

CONCLUSION

From the study carried out, it can be concluded that the characterization curves method can be adopted for characterizing atomic atomization profiles. The proposed model constitutes a new tool of clear usefulness in the characterization of the transitory signals provided by different analytical techniques.

The proposed method is capable of more clearly detecting changes in the atomization profiles than the procedure proposed by Barnett and Cooksey, probably because the proposed method uses more pairs of values $(A)_{t_i}$, t_i. Moreover, the application of this method does not require a complex mathematical tool and, therefore, the results are simpler than the model proposed by Sadler.

The results obtained with the acid treatment of the oil samples indicate that the calibration using an aqueous standard can provide accurate results. However, the use of an aqueous standard for the calibration after basic treatment of the sample can provide inaccurate analytical results, probably because of the incomplete transformation of the organometallic species of chromium into inorganic species. In addition, the use of aqueous standards provides inadequate results, even when the standard addition technique is used for calibration.

The determination of metallic elements in samples with a complex matrix (e.g., agricultural or food samples) can be carried out without complete elimination of the matrix. The analyte can be determined after extraction with an appropriate reagent or after simple dilution. Then, the analyte can be in both forms: organic and/or inorganic. Moreover, the undestroyed matrix constitutes a potential source of error. The proposed procedure is a useful tool to check if the use of aqueous standards is suitable or not in order to obtain accurate results for these kinds of samples.

ACKNOWLEDGMENTS

The authors thank the Ministerio de Ciencia y Tecnología for financial support (project BQU2002-00527).

Received May 11, 2006.

REFERENCES

1. R. Wennrich, W. Frech, and E. Lundberg, Spectrochim. Acta 4B, 239 (1989).
2. N.H.Bings, A.Bogaerts, and J.A.C.Broekaert, Anal.Chem. 74, 2691(2002).
3. B.V. L'vov; Spectrochim. Acta 56(B), 1503 (2001).
4. B.V. L'vov, Spectrochim. Acta 17, 761(1961).
5. B.V. L'vov, Spectrochim. Acta 33B, 153(1978).
6. W.B. Barnett and M.Cooksey, At. Absorpt. Newsl. 18(3,) 61 (1979).
7. J.M. Harnly, J. Anal. At. Spectrom. 3, 43 (1988).
8. W. Wegscheider, L. Jancar, M. Thai Phe, and M.R.A. Michaelis , Chem. Intell. Lab. Sys. 7, 281 (1990).
9. D.A. Sadler, P.R. Boulo, J.S. Soraghan, and D.Littlejohn, Spectrochim. Acta 53B, 821 (1998).

10. R. Calapaj, S. Chiricosta, G. Saija, and E. Bruno, At. Spectrosc. 9(4), 107(1988).

11. L.M. Costa, F.V. Silva, S.T. Gouveia, A.R.A. Nogueira, and J.A. Lóbrega, Spectrochim. Acta 56(B), 1981 (2001).

12. Z. Czövek, A. Gáspar, M. Braun, and J. Posta, Models in Chemistry 136(1–2), 95 (1999).

13. M. Llobat-Estellés, R. Marín-Sáez, and M.D. SanMartín-Ciges, Fresenius J. Anal. Chem. 342 (1992) 538.

14. D.A. Sadler, D. Littlejohn, P.R. Boulo, and J.S. Soragnan, Spectrochim. Acta 53(B), 1015 (1998).

Coupling of Multi-Pumping Flow Systems to Flame Atomic Spectrometric Detectors: Preliminary Studies and Analytical Applications in the Analysis of Biological Samples

Cristina M.P.V. Lopes, *Agostinho A. Almeida, João L.M. Santos, and José L.F.C. Lima
REQUIMTE, Departamento de Química-Física, Faculdade de Farmácia, Universidade do Porto, Rua Aníbal Cunha 164, 4099-030, Porto, Portugal

ABSTRACT

The so-called "multi-pumping flow systems" (MPFS), which rely on the utilization of solenoid-actuated micro-pumps (SAMPs) for introduction and propulsion of solutions, are a relatively recent development in the flow analysis field. They have already been coupled to several molecular spectrometric detectors with claimed advantages. However, the applicability and potentialities of their coupling to flame atomic spectrometric (FAS) detectors has never been studied.

This work describes the study of coupling multi-pumping flow systems to flame atomic absorption spectrometers (FAAS) and flame (atomic emission) photometers (FP). The main purpose was to study the behavior of SAMPs when subjected to the aspiration effect inherent to nebulizers of FAS instrumentation (Venturi effect) and to evaluate the effects of the pulsed flow, a main characteristic of MPFS, over the efficiency of the nebulization and atomization processes.

Based on these preliminary studies, several MPFS that enabled the on-line dilution of samples and/or the on-line addition of reagents (e.g., a releasing agent), two sample pre-treatment steps frequently required when using FAS detectors in analytical work, were developed. In this study, the analytical applicability has been demonstrated in the determination of Na in urine samples (using FP) and Ca and Mg in hair sample digests (using FAAS). The multi-pumping flow systems enable the configuration of simple analytical flow systems that are robust and capable of providing precise and accurate results with good sampling rates.

INTRODUCTION

The multi-pumping flow systems (MPFS) described in 2002 by Lapa et al. (1) represent an innovation in the flow analysis field. These systems are based on the utilization of solenoid-actuated micro-pumps (SAMPs) for the introduction and propulsion of solutions in a characteristically pulsed flow. In contrast to the laminar flow (which is a characteristic of most other flow systems), the pulsed flow (which promotes the chaotic movement of solutions in all directions) facilitates the mixing processes even under conditions of limited dispersion (e.g., short reactors). The advantages of the pulsed flow (2) justify the rapid acceptance of the MPFS as shown by the increasing number of scientific publications in which its coupling to diverse detector types is discussed, namely molecular absorption spectrophotometers (3), luminometers (4), and fluorimeters (5). However, the potential of coupling MPFS to flame atomic absorption spectrometers (FAAS) and flame photometers (FP) has not yet been investigated.

This kinds of instruments are capable of self-aspirating the analytical solutions (Venturi effect), thus eliminating other sample introduction devices, and sample analysis is preceded by nebulization and atomization of the solutions. Thus, it is important to establish the viability of coupling a MPFS to FAAS or FP by assessing the influence of the pulsed flow on the overall sample introduction process (aspiration - nebulization - atomization) as well as on the analytical signal obtained.

In this work, multi-pumping flow systems of simple configuration were constructed in order to evaluate their performance when coupled to FAAS (spray chamber with either a flow spoiler or an impact bead) and to a FP. The analytical applicability, precision, and accuracy were evaluated in the FAAS determination of Ca and Mg in hair sample digests (which requires not only prior dilution of the samples but also their efficient mixture with a releasing agent, such as lanthanum solution) and in the FP determination of Na in urine samples (which requires a prior and highly elevated dilution of the sample).

EXPERIMENTAL

Instrumentation

FAAS determinations were performed using a PerkinElmer® Model 5000 air/acetylene flame atomic absorption spectrometer (spray chamber with a flow spoiler) (PerkinElmer Life and Analytical Sciences, Shelton, CT, USA). In preliminary experiments, a Pye Unicam (Cambridge, UK) Model SP9 air/acetylene FAAS (spray chamber with an impact bead) was also used. Calcium and magnesium hollow cathode lamps (Cathodeon, Cambridge, UK) were used as the radiation sources.

**Corresponding author.*
E-mail: aalmeida@ff.up.pt
Tel: +351 22 208 71 32
Fax: +351 22 200 44 27

Atomic Spectroscopy
Vol. 27(5), Sept./Oct. 2006

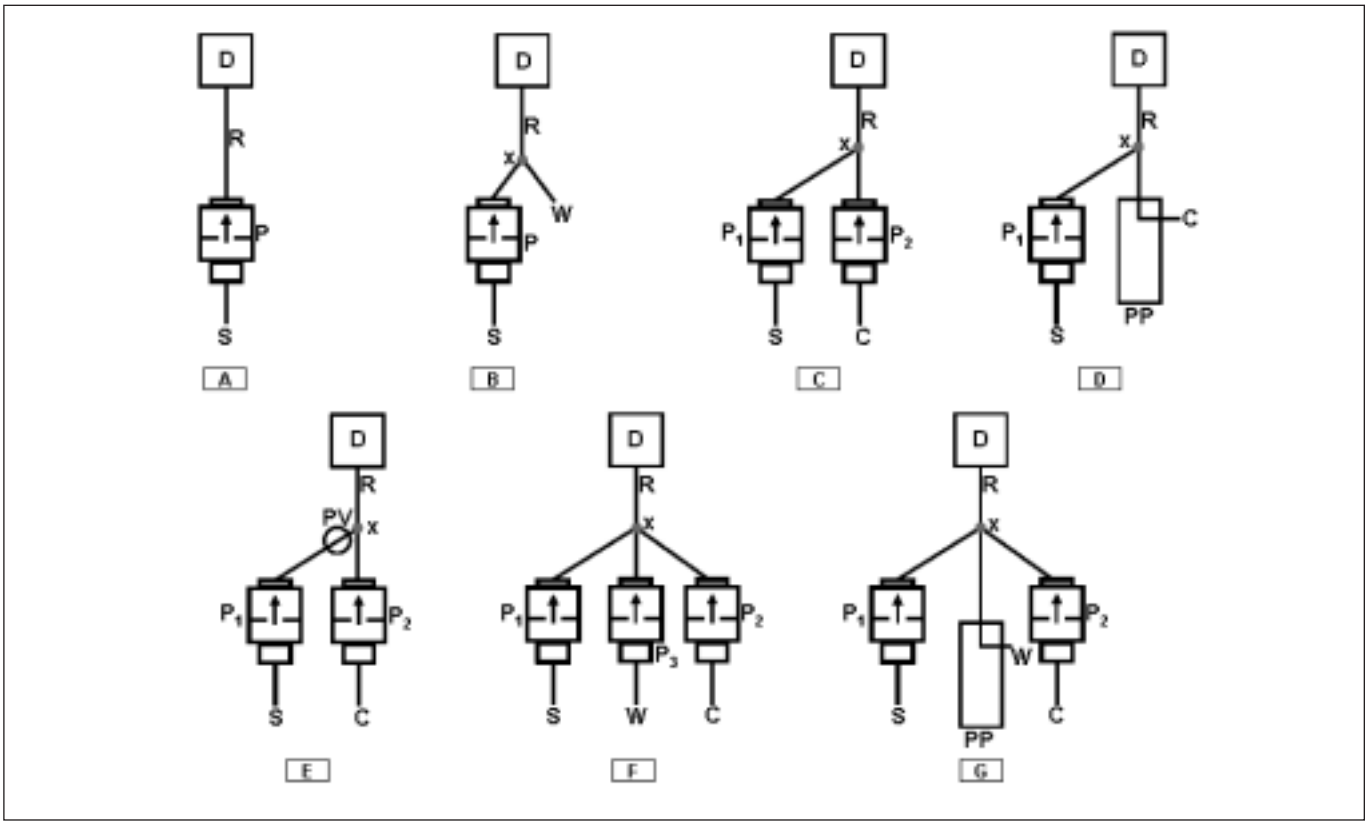

Fig. 1 (A–G). Schematic diagrams of the flow manifolds: C = carrier (water or La solution, depending on the experiments, in configuration C – see text; water in configurations D and E; La solution in configurations F and G); D = detector; P, P1, P2 and P3 = solenoid-actuated micro-pumps; PV = pinch valve; PP = peristaltic pump; R = reactor; S = sample; W = water; X = confluence point.

For FP measurements, a Buck Scientific (East Norwalk, CT, USA) Model PFP-7 air/butane flame atomic emission photometer was used. A Metrohm AG (Herisau, Switzerland) Model E 586 Labograph recorder was attached to all equipment.

The flow systems (Figure 1) were constructed using solenoid-actuated micro-pumps (Series 090SP and 120SP, from Bio-Chem Valve Inc., Cambridge, UK) capable of dispensing a fixed volume of 3, 5, 8, 25, or 50 µL per stroke (pulse), a peristaltic pump (Gilson® Model Minipuls™ 2, Villiers-le-Bell, France) with a propulsion tube (Gilson), PTFE tubes (0.8 mm i.d., Omnifit, Cambridge, UK), and home-made confluences (Figure 2) and connectors.

Flow system control as well as data acquisition and processing were carried out by means of a personal computer equipped with a Pentium®-III processor and a PCL-711B PC-MultiLab Interface Card (Advantech, Taipei, ROC). Solenoid-actuated micro-pumps were controlled by using a CoolDrive power driver circuit (NResearch Inc., West Caldwell, NJ, USA) and software was developed in Microsoft® QuickBasic® 4.5 program.

Wet acid digestions were carried out in a Model MLS-1200 Mega microwave oven equipped with HPR-1000/10 S rotor (Milestone, Sorisole, Italy).

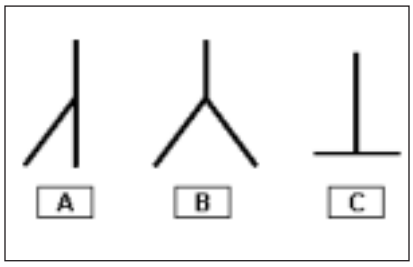

Fig. 2. Different angles tested at the confluence point X.

Reagents and Solutions

All reagents were of analytical grade (Merck, Darmstadt, Germany), unless otherwise indicated.

For FAAS determinations, the standard solutions were prepared by adequate dilution of 1000 mg L^{-1} calcium or magnesium standard stock solutions (Spectrosol®, from BDH, Poole, England) with 0.2% (v/v) HNO_3.

For FP determinations, a 100-g L^{-1} sodium standard stock solution was prepared by dissolving NaCl (Panreac, Barcelona, Spain) in 0.2% (v/v) HNO_3. Calibrating standard solutions were then prepared by adequate dilution with 0.2% (v/v) HNO_3.

Lanthanum stock solution [1000 mg L^{-1} or 0.12% (w/v)] was prepared by dissolving La_2O_3 (Sigma-Aldrich, Milwaukee, WI, USA) with 0.6% (v/v) HCl.

The hair samples were washed in 1% (v/v) Triton® X-100 solution. For digestion of the hair samples, concentrated HNO_3 and 30% (m/m) H_2O_2 solutions (Riedel-de Häen, Seelze, Germany) were used.

High quality water (resistivity >18 MΩ cm^{-1}) obtained through a Milli-Q™ system (Millipore, Bedford, MA, USA) was used in the preparation of all solutions.

To evaluate the analytical accuracy, hair (IAEA-086, Btl No. 81; from IAEA, Vienna, Austria) and urine reference samples (Seronorm™ Trace Elements Urine, lot NO2525, from SERO AS, Billingstad, Norway) were used.

Sample Preparation

Hair Samples

The hair samples were previously submitted to mechanical agitation washing with a 1 % (v/v) Triton® X-100 solution for 30 minutes. After suitable rinsing with water to eliminate the detergent, the samples were left to dry overnight in an oven at 105 ºC.

For sample wet digestion, ~0.25 g of sample plus 3 mL of concentrated HNO_3 and 1 mL of 30 % H_2O_2 were placed in the microwave oven vessels. The microwave oven program was used as recommended by the manufacturer for organic samples with rapid exothermic reactions and was comprised of five heating cycles: 1 min at 250 W; 2 min at 0 W; 5 min at 250 W; 5 min at 400 W; and 5 min at 600 W. After cooling, deionized Milli-Q water was added to the hair digests to achieve a final volume of 15 mL. In each digestion cycle, a microwave oven vessel was used for the reference sample and another one to act as the sample blank.

For Ca and Mg determinations by the manual procedure (for comparison with the results obtained by the proposed flow system), the hair digests were diluted 1+14 with deionized water.

Urine Samples

Urine samples were collected in polyethylene containers, acidified to pH < 2 with nitric acid, and stored in a refrigerator at 5 °C until analysis. Some were spiked with small volumes of a sodium standard solution. Prior to analysis, the samples were shaken vigorously and centrifuged at 4000 g for 5 minutes.

For the Na determinations using the manual procedure (for comparison with the results obtained by the proposed flow system), the urine samples were diluted 1+199 with deionized water.

Flow Systems

Determination of Ca and Mg in Hair Digests

The schematic diagram of the flow system used for Ca and Mg determinations in hair digests is depicted in Figure 1(G). The analytical cycle started with first cleaning the sample channel. For this purpose, 60 µL of sample S (i.e., 20 pulses of 3 µL) was introduced into the flow system by activating SAMP P1 at a pulse frequency of 300 pulses min^{-1} (pulse interval of 0.2 s), followed by a 10-s period in which only the peristaltic pump PP operated. After that, 24 µL of sample S (8 pulses x 3 µL) and 400 µL of lanthanum solution C (8 pulses x 50 µL) were introduced by simultaneous activation of SAMP P1 and SAMP P2, both functioning at a pulse frequency of 100 pulses min^{-1} (pulse interval of 0.6 s). The mixture of sample S with the lanthanum solution started at confluence point X ("merging zones") and continued along the 180-cm reactor R towards detector D. During the complete analytical cycle, peristaltic pump PP continuously introduced water W through confluence point X at a 5-mL min^{-1} flow rate.
(Note: The nominal flow rate of the atomic absorption spectrometer, i.e., its free uptake, was adjusted to 4 mL min^{-1}.)

Determination of Na in Urine

The schematic diagram of the flow system used to perform Na determination in urine samples is represented in Figure 1(E). This analytical cycle also started with first cleaning the sample channel, which comprised the introduction of 60 µL of sample S (20 pulses x 3 µL) into the flow system by simultaneous activation of SAMP P1 (pulse frequency of 300 pulses min^{-1}) and the pinch valve, followed by SAMP P2 activation, to introduce 50 pulses of the carrier (water; 50 pulses x 50 µL) at a

Atomic Spectroscopy
Vol. 27(5), Sept./Oct. 2006

pulse frequency of 300 pulses min^{-1}. Then, 24 mL of sample S (8 pulses x 3 µL) was introduced by simultaneous activation of SAMP P1 (operating at a pulse frequency of 100 pulses min^{-1}) and the pinch valve. During the whole analytical cycle, SAMP P2 continually introduced carrier C (water) at a pulse frequency of 200 pulses min^{-1} (pulse interval of 0.3 s), except during introduction of sample S, where it was operated at a pulse frequency equal to SAMP P1 (100 pulses min^{-1}). The dilution of sample S in the carrier C (water) took place primarily at confluence point X (SAMP P1 and SAMP P2 presented internal volumes of 3 µL and 50 µL, respectively), continuing thereafter by dispersion of sample S in the carrier C along reactor R (180 cm length) towards the detector D. (Note: The nominal flow rate of the flame photometer, i.e., its free uptake, was adjusted to 4 mL min^{-1}.)

RESULTS AND DISCUSSION

Preliminary Studies

In order to achieve better understanding of SAMP operation when coupled to atomic spectrometry instrumentation, several studies were first carried out. The flow systems shown in Figure 1(A) and 1(B) were coupled to FAAS with a flow spoiler in the spray chamber; FAAS with an impact bead in the spray chamber; and FP; and the following parameters were studied: Length of reactor R (between 10 and 90 cm), the internal volume of SAMP P (between 8 and 25 µL) and its pulse frequencies (between 300 and 24 pulses min^{-1}, i.e., pulse intervals between 0.2 and 2.5 s). For each combination of these experimental conditions, the analytical signal obtained with a 2.5-mg L^{-1} Ca standard solution (prepared with a 10-mg L^{-1} La solution), in the case of FAAS, and with a 3 mg L^{-1} Na standard solution, in the case of FP, was evaluated. In each of these experiments, the flow rate produced by the SAMP was also evaluated. It was verified that whenever the SAMP was programmed to produce a flow rate lower than the nominal flow rate of the equipment, the actual flow rate produced by the SAMP was greater than the theoretically expected flow rate. In fact, during the time period defined for the activation of the solenoid during the pulse interval (pulse interval = solenoid activation time + solenoid stoppage time), aspiration of the solution by Venturi effect occurred. This difference between the expected and the actual flow rate produced by the SAMP increased with an increase in the difference between the nominal flow rate of the equipment and the flow rate theoretically expected from the operation of the SAMP. This control exercised by the equipment over the flow rate produced by the SAMP was not verified in the flow system shown in Figure 1(B), in which there was a compensation of the flow rate produced by the SAMPs through free aspiration of water at the confluence point X.

With regard to the possible effect that the pulsed flow could have on the process of nebulization/atomization, it was verified that it was constant since the analytical signals (profile and peak height) did not significantly change during the total time period of continuous introduction of the standard solutions. When SAMPs of greater internal volume, lower pulse frequencies, and/or shorter reactors were used, the effect of the pulsed flow was observed in the profile of the analytical signal, which started to present a "serrated" profile, as shown in Figure 3.

The flow system shown in Figure 1(C) enabled to evaluate the effect that the intercalation of different volumes of sample (varying the number of pulses produced by SAMP P1) in the carrier had on the analytical signal. SAMPs of different internal volumes were tested to

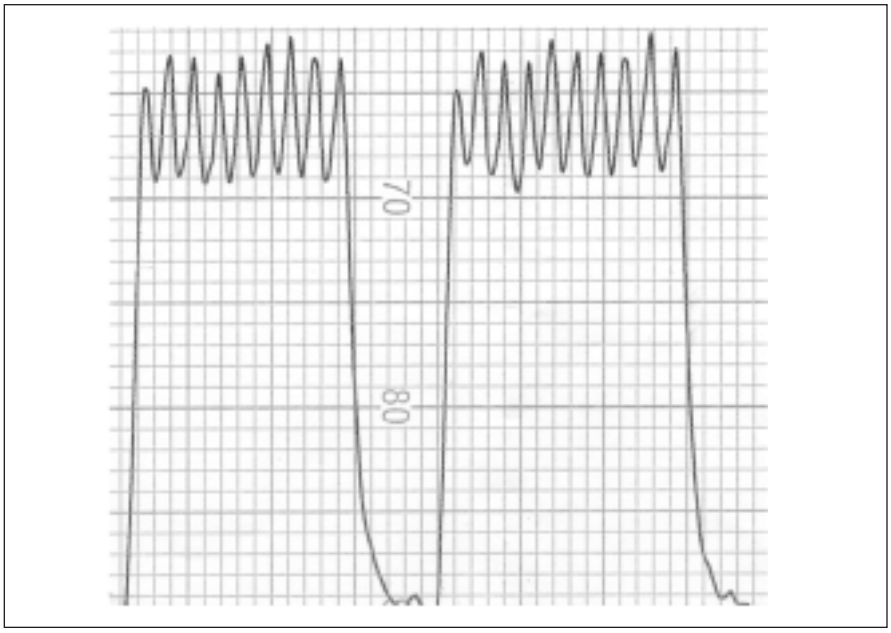

Fig. 3. Analytical signal obtained during continuous propelling of a 2.5-mg L^{-1} Ca solution using a 50-µL SAMP (pulse frequency of 100 pulses min^{-1}) through a 90-cm reactor towards the detector (FAAS).

introduce sample S (SAMP P1: 8–25 µL) and carrier C (i.e., water) (SAMP P2: 25–50 µL). We also studied different pulse frequencies for each SAMP (for SAMP P1: 150–300 pulses min^{-1} and for SAMP P2: 24–300 pulses min^{-1}), different volumes of sample S (SAMP P1: 2–40 pulses), reactors R of different lengths (90–180 cm), different angles at confluence point X (see Figure 2), and different modes of intercalating the sample in the carrier (single sample plug, merging zones, and binary sampling).

By coupling flow system 1(C) to the FAAS with a flow spoiler in the spray chamber and to the FP, highly reproducible analytical signals were obtained. Moreover, it was possible to establish a linear relationship between the volume of the sample introduced into the flow system and the analytical signal obtained. It was concluded that for the two above-mentioned atomic spectrometry systems, the pulsed flow had no significant effect in the process of nebulization/atomization, nor did aspiration by the Venturi effect influence the volume introduced by the SAMPs differently. Precision was low with the FAAS with an impact bead in the spray chamber; thus, no further studies were performed with this equipment.

It was also possible to verify that the confluence angle of the sample with the carrier, the pulse frequency of SAMP P1 (sample), and the different modes of introducing the sample into the flow system did not significantly affect the analytical signal. However, a slight increase in precision was observed when comparing binary sampling or merging zones sampling with the introduction of a single sample plug, which could be related to a more efficient mixing of the sample in the carrier.

The utilization of lower pulse frequencies (greater pulse intervals) for SAMP P2, responsible for the introduction of carrier C (water) into the flow system, resulted in an increased dispersion of sample S and, consequently, lower analytical signals without affecting precision. As was observed for the continuous sample introduction, it also holds true in this case (the intercalation of a single sample plug in the carrier): When using SAMPs of greater internal volume, lower pulse frequencies, and/or shorter reactors, the effect of the pulsed flow becomes apparent in the profile of the analytical signal, which showed a "serrated" profile (Figure 4).

The precision in the introduction of micro-volumes of solutions inherent to SAMPs, together with the possibility of selecting their internal volume (pulse volume), makes the use of these devices quite attractive to carry out on-line dilutions. SAMPs enable the construction of simple manifolds (i.e., manifolds with fewer active devices) and, for this reason, they are more reliable and more robust. Sample dilution is frequently necessary in atomic spectrometry analysis not only in order to adjust the analyte concentration to the instrumental linear range, but also to minimize potential matrix effects (a common problem in the analysis of biological samples). Therefore, the flow system shown in Figure 1(C) was used as a starting point to evaluate whether the MPFS was an advantageous alternative to other flow systems (6).

A SAMP P1 of 3 µL/pulse, a SAMP P2 of 50 µL/pulse, and standard solutions of Ca 100 mg L^{-1} (for FAAS with flow spoiler) and Na 100 mg L^{-1} (for FP) were used. The following experimental parameters were tested: (i) pulse frequencies for each SAMP (75–300 pulses min^{-1}); (ii) sample volumes (3–30 µL); (iii) reactor lengths R (100–300 cm); (iv) sampling modes (binary sampling and merging zones sampling). All combinations studied showed low precision (%RSD 8.23–10.51, n = 10).

Modifications in the configuration of flow system 1(C) were made (e.g., substitution of confluence X for a three-way solenoid valve or the inclusion of a mixing chamber) but imprecision of the results was maintained. This imprecision was possibly related to the "dragging" of small dead volumes of sample by the carrier propelled by SAMP P2 and can be explained on the basis of the multi-pumping concept itself. When the solenoid valve is deactivated and the SAMP propels the solution into the flow system at a very high instantaneous velocity, chaotic movement of the solutions

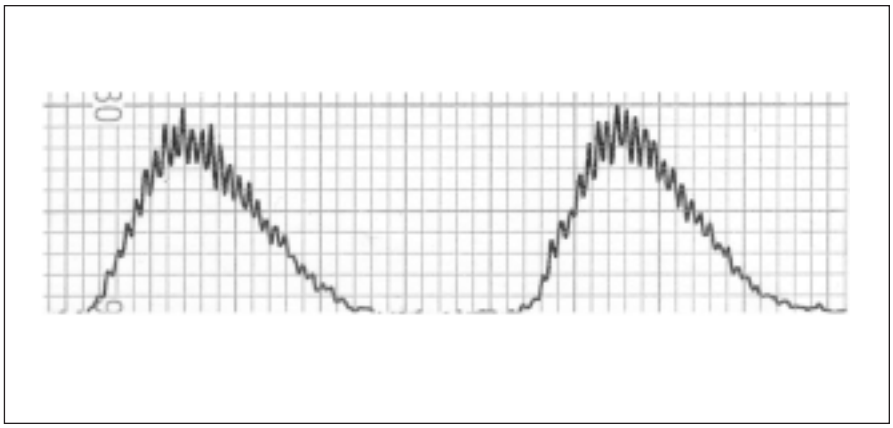

Fig. 4. Analytical signals obtained for the introduction into the flow system of single sample plugs (10 pulses of 25 µL of a 2.5 mg L^{-1} Ca solution) propelled with water through a 180-cm reactor towards the detector (FAAS) using two 25-µL SAMP operated at a pulse frequency of 100 pulses min^{-1}.

occurs in all directions. This is more evident in flow systems intended to perform the on-line dilution of highly concentrated samples.

Modifications that improved the precision of the results were as follows: (i) Replacement of SAMP P2 by a peristaltic pump, which causes less turbulence while propelling the carrier (laminar flow) – Figure 1(D) (%RSD 1.09; n = 10) and (ii) inclusion of a pinch valve between SAMP P1 and confluence X, which closed each time SAMP P2 was activated, thus avoiding the sample's channel "washing" – Figure 1(E) (%RSD 1.10; n = 10). It should be emphasized that configurations 1(C) and 1(E) increased the sensitivity (signals of higher magnitude), which could be related to an increase in the nebulization efficiency promoted by the pulsed flow.

In flame atomic spectroscopy, apart from carrying out a dilution, the addition of an ionization buffer or a "releasing agent" solution is also frequently necessary (e.g., the determination of Ca by FAAS requires the addition of a La solution to samples and standards). The utilization of configurations in Figure 1(C)–1(E) would require those solutions to be used as the carrier, thus causing a great spending of reagent. Therefore, to minimize this expenditure and to generate effluents with less environmental effect, a confluence with an additional channel that enabled the carrier to be a different solution (e.g., water), was used [Figure 1(F)].

The following options were tested: (i) SAMP P1 of 3 µL (sample); (ii) SAMP P2 of 50 µL (La solution of 1000 mg L-1), (iii) SAMP P3 of 50 µL (carrier – water); and (iv) reactor R of 180 cm length. Eight pulses of sample and eight pulses of La solution were introduced into the flow system by simultaneous activation of SAMP P1 and SAMP P2 (merging zones) at a pulse frequency of 100 pulses min^{-1}. Then, SAMP P3 was activated (pulse frequency of 200 pulses min^{-1}) and the mixture was directed towards detector D (FAAS). The linearity and precision for 10 consecutive readings of Ca standard solutions with concentrations ranging from 5 to 50 mg L^{-1} were evaluated. A calibration function Y = 0.2971 X + 0.2006 (r = 0.9999; n = 4) with %RSD values ranging from 5.39 (for the 5 mg L^{-1} solution) to 10.62 (for the 50 mg L^{-1} solution) was obtained. The precision was improved by replacing SAMP P2 (carrier introduction) with a peristaltic pump PP [Figure 1(G)]. This resulted in a calibration function of Y = 0.1342 X + 0.2579 (r = 0.9999; n = 4), with %RSD values ranging from 1.33 (for the 5-mg L^{-1} solution) to 2.89 (for the 50-mg L^{-1} solution). These %RSD values increased as the concentration of the Ca standard solution increased, confirming the "dragging" of sample small dead volumes inside the flow system, which becomes more evident as the concentration of the sample increases. As previously indicated for configurations in Figure 1(C) – 1(E), configuration 1(F) (only with SAMP) gave rise to signals of greater magnitude.

Analytical Applications

To demonstrate the applicability of MPFS for routine laboratory analysis with flame atomic spectrometry instrumentation and to evaluate precision and accuracy of the results obtained, the determination of Ca and Mg in hair sample digests (by FAAS) and Na in urine samples (by FP) was performed.

Determination of Ca and Mg in Hair Sample Digests

The concentration of Ca and Mg in hair digests can be adjusted by controlling the mass of sample that is digested and/or the final volume of solution obtained. However, since it is also usually intended to determine trace elements in those digests, it is advisable to obtain more concentrated solutions and to perform a subsequent dilution to determine the major elements.

From all of the configurations studied, those presented in Figure 1(F) and 1(G) could be better applied to the determination of Ca and Mg in the hair digests since, apart from carrying out dilution of the samples, they also enabled the on-line addition of the La solution. As previously indicated, precision was lower with configuration in Figure 1(F) (only SAMP) and, for this reason, configuration 1(G) was chosen. Some of the flow system parameters were optimized in order to improve the analytical features (precision, accuracy, and sample throughput). The studied parameters were: Length of reactor R; volume and flow rate of sample S and La solution C; concentration of the La solution C; and flow rate produced by the peristaltic pump PP.

Reactor lengths of 110, 150, 180, and 230 cm were studied. For each of these reactors, different volumes of sample S (6 and 8 pulses of 3 µL – SAMP P1) and La solution C (6 and 8 pulses of 50 µL – SAMP P2) were tested, both introduced into the flow system by the merging zones technique (i.e., simultaneously). For all of these combinations, the precision of the analytical signal was not affected by the number of pulses of SAMP P1 and P2 and increased with an increase in length of reactor R, which could be related to a decrease of the nebulizer aspiration effect in the flow system.

Different pulse frequencies (300–75 pulses min^{-1}) for SAMP P1 and P2 were tested, corresponding to different flow rates for introduction of sample and La solution. Although precision of the analytical signal (%RSD values) did not vary significantly (1.34–1.82, n = 10), it was greater for a pulse frequency of

100 pulses min^{-1} and decreased for the other pulse frequencies tested. The magnitude of the analytical signal decreased with a decrease in pulse frequency. These variations in precision and sensitivity can be explained by the variations in the solution flow rate. By increasing the pulse frequency (higher flow rates), the precision of the stroke volumes propelled by the SAMP decreases due to an increase in backpressure. On the other hand, as the same total volume is introduced into the flow system over a shorter period of time, there is not enough time for the chaotic movement of the solution inside the flow system to be "absorbed". It seems that the pulsed flow predominates over the laminar flow, resulting in a decrease of the axial dispersion and, consequently, in signals of greater magnitude. For lower pulse frequencies, due to the increase in time between each pulse, the dispersion of the sample in the carrier increases, resulting in lower signals. Additionally, these signals presented lower precision, probably due to a less reproducible dispersion.

SAMP P2 with different internal volumes (5 – 50 µL) was tested. The magnitude of the analytical signal increased with a decrease in the SAMP's internal volume, but precision decreased (e.g., for a SAMP of 5 µL: peak height = 17.67 cm and %RSD = 11.40; for a SAMP of 50 µL: peak height = 6.96 cm and %RSD = 1.0; n = 10). This must be related, respectively, to a decreased dilution at the confluence point X and changes in the Ca/La relationship, which is due to a decrease in the volume of La solution introduced into the flow system.

Lanthanum solutions of different concentrations (10 – 1000 mg L^{-1}) were tested. For each of these solutions, a calibration curve in the Ca concentration range of 5–50 mg L^{-1} (n = 4) was obtained. The average value of the %RSD values for five consecutive readings of each standard solution increased when the concentration of La solution decreased (1000 mg L^{-1}: %RSD = 0.94; 10 mg L^{-1}: %RSD = 3.29) and the correlation coefficient (r) for each calibration curve decreased (1000 mg L^{-1}: r = 0.9996; 10 mg L^{-1}: r = 0.9978).

The effect of the water W flow rate (carrier; propelled by peristaltic pump PP) on the analytical signal (magnitude and precision) was also evaluated. In the range of 2 – 5 mL min^{-1}, the sensitivity increased with a decrease in flow rate, which could be related to a lower dilution effect on sample S. The %RSD values for successive determinations (n = 10) of Ca standard solutions ranged between 2.15 – 4.56 (5 mg L^{-1}) and between 0.85 – 2.86 (50 mg L^{-1}), showing an increase as the water flow rate decreased. This is possibly due to the increased difference between the total flow rate of the flow system and the nominal flow rate of the nebulizer of the FAAS.

The effect of sample volume introduced into the system (i.e., number of pulses) on the accuracy of the results was evaluated through the analysis of a reference sample (IAEA-086, Hair, Btl. No. 81). Using different Ca standard solutions (5 – 100 mg L^{-1}) and varying the number of pulses between 2 and 10, increasing by one point (SAMP P1 of 3 µL), different calibration curves were obtained. It was verified that, although the correlation coefficient decreased as the number of sample pulses increased (2 pulses: 0.9996; 10 pulses: 0.9983), concentration values within the certified interval were only obtained for more than 8 sample pulses (i.e., sample volume ≥ 24 µL).

A SAMP P1 of greater internal volume (5 µL) was also tested in order to evaluate whether it was possible to reduce the time spent in the introduction of the sample without hindering the analytical features of the flow system. It was verified that the introduction of five sample pulses (5 x 5 µL = 25 µL) resulted in a decrease in precision and accuracy. This could be related to possible deviations in the volume actually dispensed by SAMP P1 in comparison to its nominal internal volume since for the same total volume, a SAMP P1 of 5 µL has to propel a lower number of pulses into the flow system.

The experimental parameters fixed during optimization for Ca determination in hair digests were subsequently re-evaluated for the determination of Mg. No significant differences were observed over the whole range of conditions that represented the best compromise among precision, accuracy, and analytical throughput. Therefore, the same flow system configuration was used for both elements: (i) Reactor R of 180 cm; (ii) 8 sample pulses (SAMP P1 internal volume = 3 µL); (iii) 8 pulses of a 1000-mg L^{-1} La solution (SAMP P2 internal volume = 50 µL); (iv) introduction of the sample by merging zones; (v) SAMP P1 and SAMP P2 pulse frequency of 100 pulses min^{-1}; and (vi) peristaltic pump PP flow rate of 5 mL min^{-1}.

The proposed flow system enabled precise results to be obtained, with %RSD values (n = 10) always lower than 1.98 (Ca) and 2.05 (Mg), and a good sampling rate (106 determinations $hour^{-1}$). The accuracy assessment, made by comparison of the results obtained in the analysis of the hair digests (n = 27) using the developed MPFS and the conventional procedure (manual dilution) and through the analysis of a reference sample (Tables I and II), showed that the proposed flow system provides accurate results for these analytical applications.

Determination of Na in Urine Samples

Sodium normal concentration in urine varies both with the state of hydration of the organism and the daily dietary uptake. However, it is always necessary to carry out a prior sample dilution to adjust Na concentrations to the instrumental linear range. Taking into account the results previously described (both in preliminary studies and in Ca and Mg determination), the configuration presented in Figure 1(E) was selected and adapted for this application: (i) Reactor R of 180 cm; (ii) SAMP P2 of 50 µL for the continuous introduction of the carrier/diluent C (water); (iii) SAMP P1 of 3 µL for the introduction of eight pulses of sample by merging zones with the carrier, and (iv) a pulse frequency of 100 pulses min^{-1} for SAMP P1 and SAMP P2 during sample introduction, and 200 pulses min^{-1} for SAMP P2 for the remaining time.

With the proposed flow system, a sampling rate of 105 determinations/h^{-1} was achieved. Good precision was obtained as is shown by the %RSD values for the successive determinations (n = 10) of Na standard solutions: 1.55% (250 mg L^{-1}), 1.53% (1500 mg L^{-1}), and 0.51% (7500 mg L^{-1}). Accuracy assessment, made by comparing the results obtained in the analysis of urine samples (n = 18) using the developed MPFS and the conventional procedure (manual dilution), and through the analysis of a reference sample (Tables I and II), showed that the developed flow system provides accurate results for this analytical application.

CONCLUSION

This work demonstrates the viability of coupling "multi-pumping flow systems" (MPFS) [i.e, flow systems based on the utilization of solenoid-actuated micro-pumps (SAMP) as solutions introduction and propelling devices] to flame atomic spectrometry equipment. This coupling presents the advantage of promoting efficient mixing of the analytical solutions.

The analytical features of the proposed MPFS highlighted the reproducible behavior of SAMPs in the introduction of micro-volumes of solutions, a very useful characteristic when they are used in on-line dilution flow systems. Additionally, it has been shown that MPFS can be very simple flow manifolds and provide precise results with good sampling rates.

TABLE I
Results Obtained in the Determination of Ca and Mg (Hair) and Na (Urine) in Reference Samples

Hair (FAAS) Ca ($mg.Kg^{-1}$) Obtained Results (mean ± sd; n = 5)		Reference Value	Hair (FAAS) Mg ($mg.Kg^{-1}$) Obtained Results (mean ± sd; n = 5)		Reference Value	Urine (FP) Na ($mg\ L^{-1}$) Obtained Results (mean ± sd; n = 5)		Reference Value
MPFS	Manual Procedure	1120 ± 120	MPFS	Manual Procedure	177 ± 21	MPFS	Manual Procedure	2545 ± 82
1122 ± 136	1121 ± 152		171 ± 12	176 ± 18		2532 ± 42	2585 ± 45	

FAAS – flame atomic absorption spectrometry; FP – flame photometry; MPFS – multi-pumping flow system.

TABLE II
Comparison of Results Obtained in the Determination of Ca and Mg (Hair) and Na (Urine) by the Proposed Procedure and the Conventional (Manual) Procedure

	Hair (FAAS) (n = 27) Ca	Mg	Urine (FP) (n = 18) Na
Linear Regression Equation	y = 0.999 X + 1.432	y = 0.999 X + 0.007	y = 1.002 X – 1.057
(Correlation Coefficient)	(r = 0.9998)	(r = 0.9992)	(r = 0.9997)
RD%[a] (minimum; maximum)	–1.29 ; +1.26	–4.25 ; +5.92	–3.93 ; +4.41
Paired Student's *t*-test[b]	0.51	0.14	0.56

[a] Relative deviation (%) of the results obtained by the developed procedure versus the manual procedure.
[b] Tabulated values for a two-tail paired Student's *t*-test at a 95% confidence level are 2.06 (n = 27) and 2.11 (n=17).

This type of flow system makes common sample pre-treatments (such as prior dilution and/or reagent addition) easier to carry out, and provides an economic alternative for the automation of these tasks.

ACKNOWLEDGMENTS

Cristina M.P.V. Lopes thanks FCT and FSE (III Quadro Comunitário de Apoio) for a PhD Grant (BD/5967/2001).

Received April 12, 2006.

REFERENCES

1. R.A.S. Lapa, J.L.F.C. Lima, B.F. Reis, J.L.M. Santos, and E.A.G Zagatto, Anal. Chim. Acta 466, 125 (2002).
2. J.L.F.C. Lima, J.L.M. Santos, A.C.B. Dias, M.F.T. Ribeiro, and E.A.G. Zagatto, Talanta 64, 1091 (2004).
3. Josiane M. Toloti Carneiro, Ana Cristi B. Dias, Elias A.G. Zagatto, João L.M. Santos, and José L.F.C. Lima, Anal. Chim. Acta 531, 279 (2005).
4. Karine L. Marques, João L. M. Santos, and José L. F. C. Lima, Anal. Bioanal. Chem. 382, 452 (2005).
5. Paula C.A.G. Pinto, M. Lúcia M.F.S. Saraiva, João L.M. Santos, and José L.F.C. Lima, Anal. Chim. Acta 539, 173 (2005).
6. J.F. Tyson, Spectrochimica Acta Rev 14, 169 (1991).

Preconcentration of Total Inorganic Selenium (Selenite and Selenate) in Natural Waters Using Zero-Valent Iron and Determination by GFAAS

S.V. Rao and *J. Arunachalam
National Center for Compositional Characterization of Materials (CCCM)
Bhabha Atomic Research Centre
Department of Atomic Energy, ECIL Post, Hyderabad–500 062, India

ABSTRACT

The applicability of inexpensive iron filings (zero-valent iron) for the preconcentration and determination of total inorganic selenium (selenite and selenate) in natural waters was investigated. Optimization studies for pH, amount of iron filings, and the extraction procedure were carried out. These studies showed that both selenium species, Se(IV) and Se(VI), could be preconcentrated using zero-valent iron in the pH range of 1–7. Quantitative recovery of total selenium (IV and VI) was achieved in a single-step extraction using a 0.4% NaOH + 0.1% Na_2SO_3 solution and determined by GFAAS. The detection limit for Se was found to be 0.06 ng mL^{-1} by GFAAS with a preconcentration factor of 30. The proposed method was applied successfully for the determination of inorganic selenium in various spiked and natural waters; the recoveries were found to be better than 95% in all cases.

INTRODUCTION

Metals and metalloids are present in trace and ultra-trace quantities in environmental matrices. These trace elements are essential micronutrients and have a variety of bio-chemical functions in all living organisms. Some of them are an integral part of several enzymes. Selenium (Se) is one such element, which is part of the glutathion peroxidase enzyme that prevents damage to cells by oxygen radicals. Thus, Se inhibits carcinogenisis by acting as antioxidant (1). Deficiency in Se also has been associated with keshan disease (2) and cardiomyopathy (3). Though selenium is an essential element, it can be toxic when taken in excess causing selenosis. Signs of selenosis include loss of hair and nails, skin lesions, tooth decay, and abnormalities of the nervous system (3,4). Hence, information on the intake and levels of Se present in environmental matrices is important in assessing the risk to human health. In environmental matrices, water is one of the main sources of selenium entering the human body. But water bodies are contaminated with Se by discharges from industrial processes (5), including coal, noble metal mining, and petroleum refining, as well as from other important sources such as agricultural irrigation of seleniferous soils. Therefore, an analysis of water for Se content is necessary to establish whether the levels of Se present are either higher or lower than permissible or required.

Estimation of selenium in water by any analytical instrument is difficult since most of the time the Se levels are less than the instrument's detection limits. Hence, an analytical method with sufficient sensitivity is required for the accurate determination of Se. Therefore, to improve analytical sensitivity, preconcentration methods using solvent extraction (6,7), ion exchange (8,9), and inorganic or organic sorbent materials (10,11) have been reported.

In water, selenium exists mainly as selenite (SeO_3^{2-}) and selenate (SeO_4^{2-}) whose oxidation states are (IV) and (VI), respectively. Little is still known on the bioavailability of either form of Se. So far, the World Health Organization (WHO) also has not changed the guidelines with respect to species. According to WHO guide lines, the limit for total Se content is 10 ng/mL. Many hyphenated analytical techniques have been developed for the determination of these species (12), but there is still the need for a cost-effective method in the determination of total selenium in water.

A large number of sorption processes for the removal of selenium and arsenic from process and wastewater have been developed. Sorbents that were mainly used for the removal of Se and As were alumina, activated carbon, and iron. Zero-valent iron is an effective and inexpensive material for the removal of heavy elements from water (13–18.). Fe(0) has been used to remove copper, silver, and mercury in water through electrochemical reduction of the cations to their elemental form (15). Murphy (17) reported that Se(VI) was removed by Fe(0) through the formation of Se(0). Rao et al. (19) reported that Se(IV) coprecipitated with Fe(III) hydroxide. However, there are no reports found in the literature where Fe(0) is used for the preconcentration and determination of ultratrace levels of selenium in water. In this study, we investigated a method for the preconcentration of Se on iron filings and its determination after recovery using a graphite furnace atomic absorption spectrometer (GFAAS).

**Corresponding author.*
E-mail: aruncccm@rediffmail.com
Tel: +91-40-27121365
Fax: +91-40-27125463

EXPERIMENTAL

Instrumentation

A Model ZEEnit 65 graphite furnace atomic absorption spectrometer (GFAAS), equipped with an MPE 60 autosampler, was used for the determination of Se at the ng mL^{-1} levels (Analytikjena, Jena, Germany). The spectrometer was provided with both the Zeeman- (transverse variable magnetic field) and deuterium-HCL-based background correction systems. The Zeeman background correction with magnetic field of 1 Tesla (2-field) was used throughout this work. A hollow cathode lamp (GBC, Dandenong, Australia) was used as the light source, which was operated at 8 mA current. The spectral band pass of 1.2 nm and a wavelength at 196.0 nm were used. Analytikjena pyrolytically coated graphite tubes with platform were used. A sample volume of 20 µL was injected into the furnace during analysis. $Pd(NO_3)_2$ was used as the modifier, argon gas as the purging gas, and the signals were used as peak areas. The furnace conditions are given in Table I.

A laboratory model of REMI centrifuge (Mumbai, India) was used to centrifuge the solutions. All pH measurements were made with a digital pH meter (Global Electronics, Hyderabad, India).

TABLE I
Graphite Furnace Program Employed to Determine Se by GFAAS

Step	Temp. (°C)	Ramp Rate (°C/s)	Hold Time (s)
Drying	90	5	20
Drying	105	3	20
Drying	110	2	10
Pyrolysis	1100	125	12
Atomization	2100	1300	5
Cleanout	2500	500	3

Reagents

All solutions were prepared using analytical reagent grade chemicals and deionized (DI) water (Milli-Q™ water, >18MΩ cm resistivity). Stock standards (1 mg/mL) of Se(IV) and Se(VI) were prepared from Na_2SeO_3 and Na_2SeO_4 (E. Merck, Darmstadt, Germany), respectively. Working solutions of Se(IV) and Se(VI) were prepared as and when required by appropriate dilution of the stock solutions. Iron metal filings of 100 mesh size (Loba Chemie Pvt., Ltd., Delhi, India) were used. NaOH and Na_2SO_3 used for extraction purposes were obtained from S.D. Fine Chem. Pvt. Ltd., Mumbai, India. The pH of all solutions was adjusted using very dilute solutions of HCl or NaOH. The solutions of Na^+, K^+, Ca^{2+}, Mg^{2+}, Cl^-, F^-, SO_4^{2-}, PO_4^{3-}, and NO_3^- used in the study of interferences were prepared by appropriate dilution of the stock solutions of their salts.

Procedure

The experiments for the initial sorption studies of selenium on zero-valent iron filings were conducted by spiking known amounts of Se(IV) or Se(VI) or a mixture of both species in DI water. Optimization studies for pH, amount of iron filings, and for the extraction procedure were carried out. A study on the effect of other ions was also carried out. The procedure developed for the preconcentration of both selenium species (IV and VI) on iron filings and the determination of total Se by GFAAS was as follows:

A 50-mL spiked sample solution of 20 ng/mL of Se(IV) or Se(VI) or a mixture of both was taken into a 250-mL separating flask made of fluorinated ethylene propylene (FEP), and the pH was adjusted to 5.0. Iron filings of 500 mg were added to the solution. The flask was closed with a lid and manually tilted up and down for 10 minutes. Then the flask was left standing for 5 minutes. After the iron filings settled, the paste of the iron filings was drawn (by opening the stopcock) along with little solution from the outlet of the separating flask into the centrifuge tube (15 mL), made of polypropylene (PP). Then, 4.5 mL of an aqueous solution containing 0.4% NaOH and 0.1% Na_2SO_3 was added and the tube shaken manually for 10 minutes. The solution was centrifuged at ~3000 rpm for 5 minutes. The final solution was decanted into another fresh PP tube, made up to 5-mL volume by addition of 0.2 mL of concentrated HNO_3, and the solution analyzed for selenium content by GFAAS. The process blanks were prepared taking 150 mL of DI water and following the procedure as described above.

Similar experiments were conducted with real samples of ground, municipal, and lake water. In these cases, a 150-mL sample was taken since the Se levels were expected to be very low.

RESULTS AND DISCUSSIONS

Sorption of Selenium on Fe(0)

Effect of pH

Experiments were carried out at pH ranges from 1–12 with 500 mg of iron filings by taking spiked solutions (50 mL) of Se(IV) and Se(VI) separately (at the 20-ng/mL level). Upon analyzing the solution after sorption, it was found that sorption was >90% in the pH ranges of 1–7, but there was no sorption after pH 8. This trend was almost the same for both species. The optimum pH was found to be close to 5 where maximum sorption (99%) was observed for both the species (Figure 1). Sorption of Se below a pH of 7.0 may be due to the availability of an active surface of Fe(0), while above a pH of 7.0 formation of an oxide layer on the surface restricts the electrochemical reduction by iron.

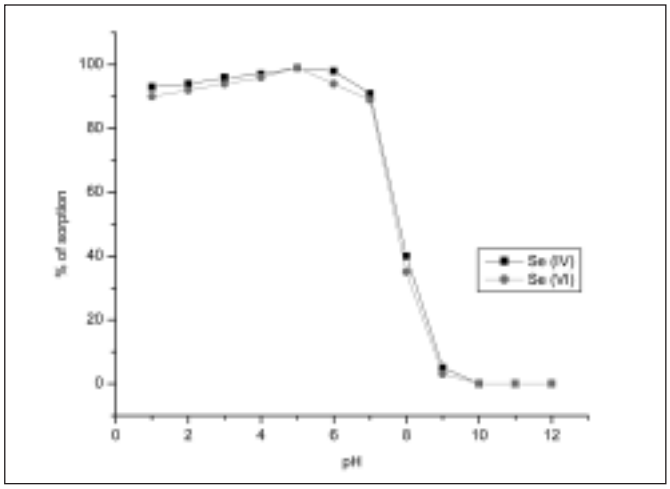

Fig.1. Effect of pH on the sorption of Se(IV) and Se(VI).

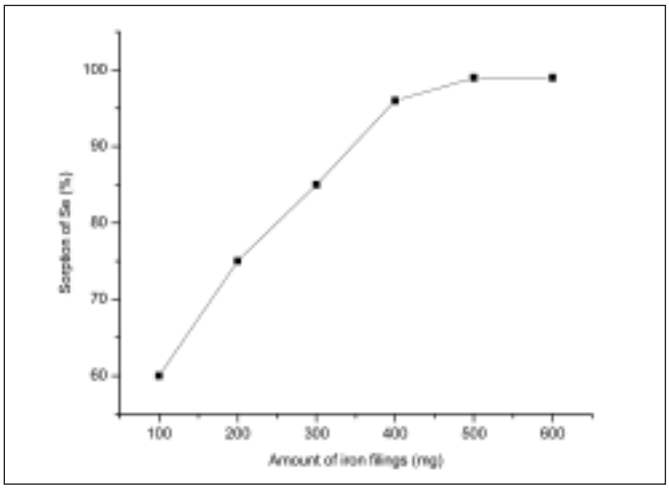

Fig.2. Effect of amount of iron filings on the sorption of Se.

Effect of Amount of Iron Filings

Experiments were carried out with different amounts (100, 200, 300, 400, 500, 600 mg) of iron filings by taking spiked solutions (50 mL) of a mixture of Se(IV) and Se(VI) (10 ng/mL each) at a pH of 5.0. It was found that maximum sorption (>99%) of selenium was taking place when the amount of iron filings was ≥500 mg (Figure 2). The time fixed for these experiments was 10 minutes. In our studies, it was found that an increase in the amount of iron filings makes the reaction faster since a larger surface area is then available. Hence, as a tradeoff between the amount of iron filings and time, 500 mg was fixed for further experiments, which required a moderate time of 10 minutes.

Sorption Process

Zero-valent iron was found to be a very efficient sorbent for both selenium species (IV and VI) in the pH ranges of 1.0–7.0. This is due to the electrochemical reduction of the selenium species to their elemental or selenide form. Earlier papers had reported that zero-valent iron reduces oxyanions of selenium to Se(0) and Se(-II). Roberson Mark et al. (20) reported that their X-ray absorption near-edge spectroscopy (XANES) studies revealed that selenate was reduced to elemental selenium and selenide. Meng et al. (21) reported similar findings from X-ray photoelectron spectroscopy (XPS).

Extraction of Selenium

Since sorbed selenium exists in two forms (elemental selenium and pyrite-selenium, FeSe or $FeSe_2$), extraction of these two species into a single solution was not achieved. Therefore, either a total dissolution method or a 2-step leaching of selenium was used to quantify total selenium content. Velinsky et al. (22) used a 1M Na_2SO_3 solution at pH 7.0 to extract Se(0) and Cr(II) solutions to release pyrite-selenium from sediments. Initially, we also tried to extract Se using a 1M Na_2SO_3 solution at pH 7.0. But recovery was found to be only 30–40%. This observation is similar to the findings of Meng et al. (21). They reported that the extent of elemental selenium formed was 30% whereas for selenide it was 70%. However, we used a solution of 0.4% NaOH + 0.1% Na_2SO_3 for extracting total selenium that was preconcentrated on zero-valent iron. We found that >95% of total selenium could be recovered into 4–5 mL of 0.4% NaOH + 0.1% Na_2SO_3 solution by a simple shaking for 10 minutes. It is known that elemental selenium is soluble in Na_2SO_3 by forming selenosulphate ($SSeO_3^{2-}$) (23). Solubility of ferrous selenide in Na_2SO_3 is negligible (22). In our study, it was understood that concentration of NaOH is important in the extraction of $FeSe/FeSe_2$. Experiments were carried out by keeping the Na_2SO_3 concentration at 0.1% and varying the concentration of NaOH from 0.1–0.5%. It was found that 0.4% NaOH was optimum to get >95% of the sorbed Se (Figure 3). When NaOH is <0.4%, extraction was not complete even after using >0.1% Na_2SO_3. It had been reported (24) that at a higher pH, in the presence of oxygen, sulfer undergoes oxidation in sulfidic materials such as FeS/FeS_2. The role of NaOH in leaching elemental selenium and selenides may be explained by the following reaction:

$$2FeSe(or FeSe_2) + 4NaOH + 3O_2 \rightarrow 2Fe(OH)_2 + 2Na_2SeO_3 \text{ (or } Na_2Se_2O_3)$$

$$Se + 2NaOH + O_2 \rightarrow Na_2SeO_3 + H_2O$$

At higher concentrations of sodium hydroxide, Se(0) and Se(–II) are oxidized to Se(IV) in the presence of dissolved oxygen and by coming into solution. However, the use of Na_2SO_3 is necessary as it

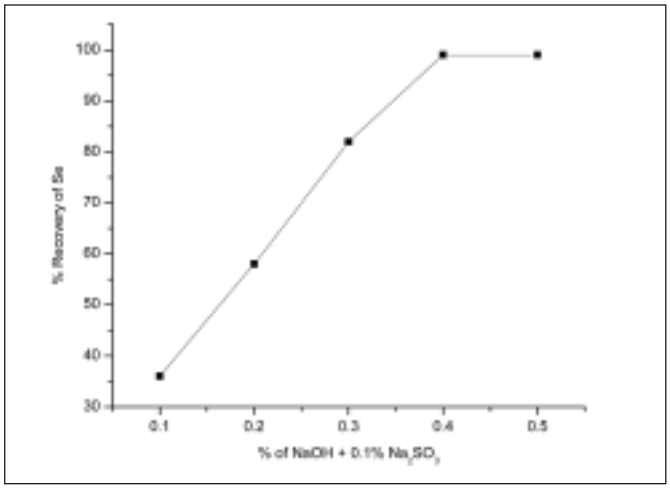

Fig.3. Effect of concentration of NaOH with 0.1% Na_2SO_3 on the recovery of total Se.

TABLE II
Determination of Selenium in Spiked Sample Solutions

Synthetic Sample	Added (ng/mL) Se(IV)	Se(VI)	Found Total Se	Recovery (%)
1	20	0	19.8±0.2	99±1
2	10	10	19.6±0.4	98±2
3	0	20	19.6±0.2	98±1

Sample Volume 50 mL; ± Standard Deviation (n=3).

may play the role of catalyst to achieve a fast reaction in solubilizing Se(0) and bringing it into the aqueous phase. By conducting experiment with 0.4% NaOH alone, Se recovery was found to be poor.

Limit of Detection and Precision of the Method

The detection limit was evaluated as the concentration corresponding to three times the standard deviation of the blank signal. The detection limit for Se was found to be 0.06 ng mL^{-1} by GFAAS, with a preconcentration factor of 30.

The precision of the determination of Se was evaluated under the optimum experimental conditions. For this purpose, three successive experiments were performed using the procedure described above with 50 mL of sample solution containing 20 ng/mL of a mixture of Se(IV) and Se(VI). These results showed a recovery of 97 ± 2% for selenium.

Effect of Foreign Ions

The interference of different ions on the sorption process is in general attributed to the strength of interaction between the ions and the sorbent. The effect of different ions such as Na^+, K^+, Ca^{2+}, Mg^{2+}, Cl^-, F^-, SO_4^{2-}, PO_4^{3-}, and NO_3^-, which are commonly encountered in waters on the sorption of selenium, was evaluated to assess the selectivity of the method. A 50-mL portion of the synthetic water sample containing 20 ng/mL of Se was spiked with various ions at different concentrations such as: Na^+ (50 µg/mL), K^+ (50 µg/mL), Ca^{2+} (50 µg/mL), Mg^{2+} (50 µg/mL), Cl^- (400 µg/mL), F^- (5 µg/mL), SO_4^{2-} (50 µg/mL), PO_4^{3-} (1 µg/mL), and NO_3^- (50 µg/mL).

These studies showed that sorption of selenium from these synthetic sample solutions was not affected in the presence of ions in the concentration range as specified in parentheses and that the recoveries were found to be in the range of 96-98%.

Analysis of Synthetic Samples and Recovery Studies

In order to demonstrate the reliability of this proposed method, experiments were carried out with water samples prepared by adding known amounts of Se(IV) and Se(VI) to Milli-Q water and applying the procedure described. The recovery of Se in all cases was found to be 98–99% (see Table II).

Analysis of Natural Water Samples

Municipal, lake, and groundwater samples were collected in precleaned polyethylene bottles in Hyderabad, India. These water samples, after adjusting the pH to 5, were analyzed using the procedure described. Concentrations of total selenium (IV and VI) determined in these samples and using the proposed method are listed in Table III. In the absence of a reference standard, known amounts of selenium [either Se(IV) or Se(VI)] were added to these samples and the recoveries obtained were found to be above 95% (Table III).

CONCLUSION

Iron filings (zero-valent iron), an inexpensive material, was found to be very effective for the preconcentration of inorganic selenium (selenite and selenate) in natural waters. These studies indicate that both selenium species, Se(IV) and Se(VI), were sorbed in the pH range of 1–7. Quantitative recovery of total selenium was achieved in a single step using a 0.4% NaOH + 0.1% Na_2SO_3 solution. The proposed method was applied successfully for the determination of total Se in various spiked and natural waters and the recoveries were found to be better than 95% in all cases.

Received July 5, 2006.

TABLE III
Determination of Total Selenium in Natural Water Samples

Sample	Added (ng/mL) Se(IV)	Added (ng/mL) Se(VI)	Found (ng/mL) Present Method Total Se	Recovery (%)
Municipal Water				
	0	0	0.38±0.07	–
	5	0	5.28±0.09	98±2
	0	5	5.27±0.14	98±3
Lake Water				
(Hussain Sagar)	0	0	1.21±0.05	–
	5	0	6.03±0.11	96±2
	0	5	6.06±0.13	97±2
Groundwater				
	0	0	0.54±0.06	–
	5	0	5.44±0.15	98±3
	0	5	5.40±0.11	97±2

Sample Volume 150 mL; ± Standard Deviation (n=3).

REFERENCES

1. I.D. Capel, M. Jenner, H.M. Dorrel, and D.C. Williams, IRCS Med.Sci. 8, 382 (1980).

2. X.Chen, G.Yang, X.Chen, X.Chen, Z.Wen, and K.Ge, Bio.Trace Elem. Res. 2, 91 (1980).

3. G.Yang, K.Ge, J. Chen, and X.Chen, World Rev. Nutr. Diet 55, 98 (1988).

4. G.Q. Yang, In: Chandra R.K (Ed.), Trace Elements in Nutrition of Children, Raven Press, New York, pg. 273 (1985).

5. J.P. Skorupa, In: W.T. Frankenberger and R.A. Engberg (Ed.), Environmental Chemistry of Selenium, Marcel Dekker, New York, Ch.18, pg. 315 (1998).

6. M.N. Pathare and A.D.Sawant, Anal. Lett. 28, 317 (1995).

7. K. Suvardhan, L. Krishnaiah, K. Suresh kumar, D. Rekha, B. Jayaraj, S. Ramanaiah, and P. Chiranjeevi, Chemosphere 62, 899 (2006).

8. U. Ornemark and A. Olin, Talanta 41, 67 (1994).

9. C. Elleouet, F. Quentel, and C. Madec, Water Res. 30, 909 (1996).

10. A. Afkhami and T. Madrakian, Talanta 58, 311 (2002).

11. S. Li, N. Deng, Anal. Bioanal. Chem. 374, 1341 (2002).

12. M. Bueno and M. Potin-Gautier, J. Chromatogr. A 963, 185 (2002).

13. R.J. Baldwin, W. Acres, J.C. Stauter, and D.L. Terrell, U.S. Patent No. 4, 405, 464 (1983).

14. K.J. Cantrell, D.I. Kaplan, and T.W. Wietsma, J. Hazard. Mater. 42, 201 (1995).

15. J.P. Gould, Water Resour. 16, 871 (1982).

16. B.Gu, L. Liang, M.J. Dickey, X. Yin, and S. Dai, Environ.Sci.Technol 32, 3366 (1998).

17. A.P. Murphy, Ind. Eng. Chem. Res. 27, 187 (1988).

18. T.E. Shokes and G. Moller, Environ. Sci.Technol 33, 282 (1999).

19.T.P. Rao, M. Anbu, M.L.P. Reddy, C.S.P. Iyer, and A.D. Damodaran, Anal. Lett. 29, 2563 (1996).

20. http://natres.psu.ac.th/Link/SoilCongress/bdd/symp6/1942-t.pdf

21. X. Meng, S. Bang, and G.P. Korfiatis, Water Research 36, 3867 (2002).

22. D.J. Velinsky and G.A. Cutter, Anal. Chim. Acta 235, 419 (1990).

23. F. Feigl, V.Anger, and RE. Oesper, Spot Tests in Inorganic Analysis, Elsevier, Amsterdam, The Netherlands, pg. 408 (1972).

24. http://crcleme.org.au/Pubs/OFR165/CRCLEME_OFR165.pdf

Solvent Extraction Separation of Heavy Rare Earth Elements From Light Rare Earth Elements and Thorium: ICP-AES Determination of REEs and Yttrium in Monazite Mineral

*A. Premadas[a] and C.R. Khorge[b]

[a] Chemistry Laboratory, Southern Region, Atomic Minerals Directorate for Exploration and Research, Department of Atomic Energy, Nagarbhavi, Bangalore - 560072, India

[b] Chemistry Laboratory, Central Region, Atomic Minerals Directorate for Exploration and Research, Department of Atomic Energy, Civil Lines, Nagpur - 440 001, India

ABSTRACT

An accurate and direct ICP-AES determination of low-level heavy rare earth elements (HREEs) in Indian monazite mineral is difficult due to spectral interferences and also due to changes in the plasma excitation conditions in the presence of very high amounts of light rare earth elements (LREEs) and thorium. A solvent extraction procedure for the separation of HREEs from LREEs and Th in monazite mineral is described for interference-free ICP-AES determinations. The REE, Y, and Th content in the monazite is prepared in either 0.1M or 0.2M HCl and the HREEs are selectively separated from LREEs and Th using 0.22M bis-(2-ethyl hexyl) hydrogen phosphate (HDEHP). The complete back-extraction of the HREEs is achieved using 4M HCl in the presence of tri-butyl phosphate (TBP).

Two certified reference materials, IGS-36, Monazite Reference Sample (British Geological Survey) and SY-3, Syenite Rock (Canadian Certified Reference Materials Projects), and a synthetic mixture of REEs, Y, and Th, corresponding to the composition of the typical monazite mineral, were used to check the recovery of HREEs. The standard deviation obtained for the separation of HREEs and determination by ICP-AES, as well as the direct determination of LREEs and Y, ranged from 1-7 % (n=4). Using this procedure, a set of 12 monazite samples can be analyzed for the determination of REEs and Y in two eight-hour working days.

INTRODUCTION

Rare earth element (REE) patterns are used in geochemical studies (1,2) and in the electronic industry (3) for making super-conductors, phosphors, optoelectronics, super-magnets, lasers, computers, rechargeable hydride batteries, artificial diamonds, glass and ceramics, etc., and in the nuclear industry (4), while certain REEs (such as Gd) are used as control rods in nuclear reactors due to their high neutron absorption capacity. The Indian monazite mineral is one of the main commercial sources of REEs and Th. It is readily available in India from beach sands at Chavara in Kerala, at Manavalakuruchi in Tamil Nadu, and in certain parts of the Orissa coast. It also occurs as an accessory mineral in acidic igneous rocks and gneisses, and may be found as relatively large crystals in pegmatites (5). Indian monazites are rich in thorium and light rare earth elements (LREEs), such as La, Ce, Pr, Nd, and Sm, and poor in certain heavy rare earth elements (HREEs), such as Tb, Dy, Ho, Er, Tm, Yb, and Lu.

Inductively coupled plasma atomic emission spectrometry (ICP-AES) is a widely used technique for the determination of REEs (6–9) in geological samples and in REE concentrates (10). The technique is sensitive, simple in operation, and of moderate cost with regard to instrumentation and analysis, making it affordable in developing countries. The interelement spectral interferences encountered in REE determinations by ICP-AES have been extensively studied by Daskalova and co-workers (11–15) and the possible interferences of other REEs on the analyte line of interest have been tabulated. Rucandio (10) determined the lanthanides and yttrium in rare earth ores and concentrates by applying suitable multiple mathematical corrections using a computer program. In the ICP-AES determination of REEs, especially in concentrated samples, increased background intensities are found with increasing REE concentrations. Because many REEs have multiple-line spectra in ICP-AES, a possibility for mutual spectral interferences among the REEs exists. This requires the use of many precautions if accurate values are to be obtained. Therefore, it is often necessary to remove a major portion of the elements La, Ce, Pr, Nd, and Th present, so that their concentration in the aspirated solution is either below the interference level, or their contribution to analyte line

*Corresponding author.
E-mail: apremadas@yahoo.co.in

intensity can easily be corrected for without compromising accuracy. Besides spectral interferences, the presence of higher quantities of LREEs and Th changes the plasma excitation conditions, affecting the emission intensity of the analyte lines. With these considerations in mind, the aim of this study was to develop a method for the interference-free ICP-AES determination of REEs and Y in monazite mineral.

The monazite mineral is refractory in nature, thus creating problems in the preparation of sample solutions. The commonly used sulphuric acid fuming (16) procedure dissolves the sample (monazite mineral grain without crushing), but associated minor quantities of other heavy refractory minerals like zircon, rutile, silliminite, etc., that may also be present, are not decomposed completely. Therefore, some doubt about the representativeness of the sample solution from this procedure arises.

There are different techniques for the group separation of REEs and Y from the other constituents of the rock sample based on the similar chemical and physical behavior of these elements, including precipitation (17,18), ion exchange (19,20), and liquid-liquid extraction (21,22). However, all of these techniques separate the REEs and Y as a single group.

Bis-(2-ethyl hexyl) hydrogen phosphate (HDEHP) is a commonly used extractant for REEs (23–25). However, the extraction behavior varies with each element from La to Lu due to the individual affinity of REEs for HDEHP, the pH of the aqueous solution, as well as the concentration of the extractant. We observed that by selecting the appropriate pH and the concentration of the extractant, it is possible to separate major amounts of LREEs and Th from HREEs. A 0.22M HDEHP solution was used to selectively extract HREEs from LREEs, and the re-extracted portion was used for the ICP-AES determination of Eu, Gd, Tb, Dy, Ho, Er, Tm, Yb, and Lu. The major elements La, Ce, Pr, Nd, Sm, and Y were determined directly by ICP-AES after suitable dilution.

This paper summarizes the results obtained using solvent extraction separation of HREEs from LREEs and subsequent ICP-AES determination of all REEs and Y in monazite mineral samples.

EXPERIMENTAL

Instrumentation

The ICP-AES instrument employed was a GBC Integra XM sequential spectrometer (GBC Scientific, Australia), equipped with a computer-controlled rapid-scanning monochromator. The instrumental parameters used and the lines selected are listed in Tables I and II.

Preparation of Standards

The REE stock solutions of 1000 μg mL^{-1} were prepared from high purity oxides (99.99% or 99.999%, Johnson Matthey, Royston, Hertfordshire, UK) by dissolution in hydrochloric acid (HCl); except for cerium oxide, which was dissolved by heating in nitric acid with a few drops of hydrogen peroxide. A thorium stock solution was prepared from thorium nitrate salts (AnalR® grade) and was standardized gravimetrically using the oxalate precipitation method. Suitable dilutions of the stock standards were made

TABLE I
Operating Parameters for ICP-AES System

RF Generator	Henry Electronics, Model-2000, Crystal-controlled
Frequency	40.68 MHz
Output Power	2.0 kW
Induced Power	1.2 kW
Reflected Power	<20 W
Spectrometer	
Mounting	Modified Czerny Turner
Focal Length	75cm
Grating	1800 grooves mm^{-1}
Rules Area	52 mm x 52 mm
Dispersion	0.74 nm mm^{-1} (first order)
Wavelength Range	170-800 nm
Wavelength Repeatability	±0.002 nm
Entrance Slit	20 μm
Exit Slit	20 μm
Photomultiplier	Dual, Hamamatsu R446 and R166
Operating Conditions:	
Argon Gas Flow Rate	10 L min^{-1}
Auxilliary Gas Flow Rate	0.3 L min^{-1}
Sample Gas Flow Rate	0.5 L min^{-1}
Pump	Peristaltic 12 roller
Nebulizer	Glass concentric
Sample Uptake	1.7 mL min^{-1}
Spray Chamber	Cyclonic

with 0.5M HCl for spectral interference studies. For instrument calibration, two sets of mixed reference stock solutions were prepared containing (i) 50 μg mL^{-1} each of La, Ce, Pr, Nd, and Sm; and (ii) 25 μg mL^{-1} each of Gd, Tb, Dy, Ho, Er, Tm and 5 μg mL^{-1} each of Eu, Yb, Lu, and Y. These were further diluted 10-, 25- and 50-fold with 0.5M HCl for calibration of the instrument.

Reagents

Bis-(2-ethylhexyl) hydrogen phosphate, (HDEHP), (E. Merck, Darmstadt, Germany, >97%). A 0.1–0.4M solution was prepared in kerosene and equilibrated with 6M HCl (equal volume), then washed twice with 0.1M HCl before use (referred to as reagent A).

2-Ethyl hexyl hydrogen phosphate (E. Merck, Darmstadt, Germany). The mixture contains ~45% dihydrogen mono ethylhexyl phosphate (H2MEHP) and ~55% HDEHP. A dilute solution (10% v/v) was prepared in kerosene and treated as above (referred to as reagent B).

Tri-n-butyl phosphate (TBP) (Merck Ltd., Poole, Dorset, UK) was used as received.

Potassium bifluoride (KHF2), (Aldrich, USA), of analytical reagent grade.

All other reagents used were of either GR or AnalR grade.

TABLE II
Spectral Lines Used for Emission Measurement of REEs and Y, and the Background Correction Points Applied

Element	Wavelength (nm)	Background Correction Points (nm)
La	333.749	333.770 (+0.021)
Ce	418.660	418.682 (+0.022)
Pr	422.293	422.315 (+0.022)
Nd	430.358	430.336 (-0.022)
Sm	442.434	442.453 (+0.019)
Eu	381.967	381.988 (+0.021)
Gd	342.247	342.267 (+0.020)
Tb	350.917	350.897 (-0.020)
Dy	353.170	353.151 (-0.019)
Ho	345.600	345.619 (+0.019)
Er	349.910	349.930 (+0.020)
Tm	346.220	346.241 (+0.021)
Yb	328.937	328.955 (+0.018)
Lu	261.542	261.551 (+0.009)
Y	371.030	371.050 (+0.020)

Procedure

Step (a): Sample Decomposition

A 0.250-g (-200#) monazite sample was taken into a platinum crucible (30 mL capacity) and mixed uniformly with 1.5 g flux (a powdered, homogeneous mixture of potassium bi-fluoride and sodium fluoride in 3:1 ratio). It was fused for five minutes with occasional swirling to get a clear melt and was allowed to spread onto the sides of the crucible while cooling. Then 6 mL of 1:1 sulphuric acid was added and heated slowly to produce strong fumes of oxides of sulphur; cooled; and the contents were transferred into a beaker using water and 10 mL of 6M HCl. The contents were then boiled with 5 mL of 0.8M oxalic acid to obtain a clear solution.

Step (b): Oxalate Precipitation of REEs, Y, and Th

A 35-mL amount of 0.8M oxalic acid was added to the solution from step (a) and the pH adjusted to between 0.9–1.0 (using dilute ammonia solution). The contents were boiled and kept in a boiling water bath for one hour, filtered using Whatmann No. 540 filter paper; then the residue was washed three times using aliquots of the 0.2M oxalic acid solution. The residue from the filter paper was taken back into the original beaker using a jet of water, the filter paper rinsed with 5 mL each of HCl and nitric acid, and subsequently with water. Then 2 mL perchloric acid was added to the residue in the beaker and placed on a hot plate until generation of perchloric acid fumes stopped (fuming was done inside the fume hood connected to an efficient blower and scrubber system). The residue was then digested with 10 mL of 6M HCl and taken to dryness on the water bath. Finally, the contents were dissolved in 5 mL of 1M HCl, transferred to a 50-mL volumetric flask, and then diluted to 50 mL using de-ionized water.

Step (c): Solvent Extraction Separation of Eu, Gd, Tb, Dy, Ho, Er, Tm, Yb, and Lu from LREEs and Th

Note: Extraction at two different HCl concentrations was performed. The fraction of HREEs obtained from the 0.1M HCl medium was used to determine the concentration of Eu and Gd. The HREE fraction from the 0.2M HCl medium was used for the determination of Tm, Lu, Tb, Dy, Ho, Er, and Yb.

Suitable aliquots (20 mL each) of the oxalate precipitation solution from above were transferred into two separatory funnels (125 mL). The content of one separatory funnel was diluted to 50 mL with 0.1M HCl and the content of the other funnel was diluted with 0.2M HCl. Then 20 mL of 0.22M HDEHP (reagent A) was added to each funnel and the contents shaken for five minutes. The layers were allowed to separate (30 minutes) and the aqueous layer was collected in another separatory funnel and extracted once again using 15 mL of reagent A. The corresponding organic layers were combined and the aqueous layers were discarded. The organic layers were washed for 2 minutes once using 50 mL of either 0.1M or 0.2M HCl, respectively, depending on the initial HCl concentration, and the wash dis-

carded. Then, 10 mL of reagent B and 3 mL of TBP each were added to each of the two organic layers, mixed well, and the REEs stripped three times using 4M HCl (20 mL each, using a 2-minute shaking time). The combined aqueous strips were collected into two beakers and mixed with 10 mL of nitric acid and 2 mL perchloric acid, then placed on a hot plate until complete termination of perchloric acid fumes. The residues were digested with 5 mL of 6M HCl, dried on a water bath, and diluted to 25 mL each maintaining 0.5M HCl.

The HREE fraction obtained from 0.1M HCl medium was used for the determination of Eu and Gd after diluting the solution 5 to 10 times; the HREE fraction extracted from 0.2M HCl medium was used for the direct determination of Tm and Lu; and Tb, Dy, Ho, Er, and Yb were determined after 5- to 25-fold dilution.

ICP-AES Determination

The wavelengths used and the background correction points applied are listed in Table II. Interelement spectral interference correction (26) of Nd on Pr and Eu was applied.

Step (d): Solvent Extraction Studies With Synthetic Mixture of REEs, Y, and Th

A combined working solution (which corresponds to the REE, Y, and Th content of a typical monazite mineral) containing:
25 mg La, 50 mg Ce, 5.60 mg Pr, 22.50 mg Nd, 2.50 mg Sm, 120 µg Eu, 1750 µg Gd, 350 µg Tb, 900 µg Dy, 100 µg Ho, 125 µg Er, 40 µg Tm, 70 µg Yb, 50 µg Lu, 2500 µg Y, and 15 mg Th in dilute HCl was used for the solvent extraction studies. The parameters studied were as follows: Selection of suitable concentration of HDEHP, aqueous phase acidity, and back-extraction. The synthetic mixture solution was diluted to 50 mL, maintaining an acidity of 0.1M to 0.4M HCl in the aqueous phase, and the REEs, Y, and Th were extracted and stripped as detailed above, and determined by ICP-AES after suitable dilution.

RESULTS AND DISCUSSION

Monazite Mineral Decomposition

Fusion with a mixture of potassium bifluoride and sodium fluoride helps in the complete decomposition of the mineral, including minor quantities of the accessory minerals, such as zircon, ilmenite, rutile, silliminite and garnet, if present. Since some of the monazite minerals contain small quantities of zirconium, niobium, or tantalum, these elements were also dissolved by boiling with a small quantity of oxalic acid.

Oxalate Precipitation of REEs, Y and Th

The oxalates of REEs, Y, and Th were quantitatively precipitated at a pH of 0.9–1.0, which helped in the removal of the salts and phosphates. Removal of the phosphates was necessary, otherwise preparing a clear sample solution in 0.1M HCl is not possible for the solvent extraction separation due to the precipitation of the phosphates of REEs and Th. The recovery of HREEs was complete in the presence of large quantities of LREEs (likely to be present in monazite samples) at a pH of 0.9–1.0. The La, Ce, Nd, and Th present in the sample acts as carrier for the complete precipitation of the trace quantities of HREEs in the sample.

Analytical Line Selection and Spectral Interference Studies

Since exhaustive studies have been done on the mutual spectral interference of REEs (11–15), the most commonly used REE lines (17,19–22) were taken for this study, giving importance to lines that have good sensitivity and are free from spectral interferences. Table III shows the approximate ratio range of the oxides of La, Ce, Pr, Nd, Sm, and Th to HREEs in certain monazite minerals (obtained from different parts of India, such as Manavala Kuruchi of Tamil Nadu, Chavara of Kerala, and the Orissa coast) and in monazite reference standard IGS-36. This indicates that in case of direct aspiration of the sample (0.25 g to 100 mL dilution), the concentration of REEs and Th would be more than 1 mg mL^{-1} which would alter the plasma conditions, increase the background radiation abnormally, lead to a lowering of the emission signal, and in addition cause direct spectral overlap for most of the analytical lines. Moreover, the concentration of Ce, La, Nd, and Th present in the aspirated solution is so high that accurate results of some HREEs, especially those present at very low levels, could not be obtained by simply applying the interelement interference corrections, because in many cases the analyte spectrum at low levels was completely buried by the direct overlap of emission lines from interfering elements as well as by wing overlap. Hence, it is necessary either to remove these interfering elements completely or to reduce their concentration to a safe level.

Interference studies were carried out by scanning 100–1000 µg mL^{-1} of La, Ce, Nd, and Th; 50–200 µg mL^{-1} of Pr and Sm on the analytical wavelengths of Eu 381.967 nm, Gd 342.247 nm, Tb 350.917 nm, Dy 353.170 nm, Ho 345.600 nm, Er 349.910 nm, Tm 346.220 nm, Yb 328.937 nm, and Lu 261.542 nm. The spectral overlap (direct as well as wing) and the background intensities were assessed by comparison with the spectra of the analyte standard alone (1 µg mL^{-1} each of Gd, Tb and Er; 0.5 µg mL^{-1} each of Dy, Ho and Tm; 0.1 µg mL^{-1} each of Yb

TABLE III
Approximate Ratio Range Variation in the Oxides of La, Ce, Pr, Sm, and Th to the Oxides of Eu, Gd, Tb, Dy, Ho, Er, Tm, Yb, and Lu in Monazite Minerals[a]

	La	Ce	Pr	Nd	Sm	Th
Eu	350–750	800–3000	70–350	300–1500	50–100	170–550
Gd	15–21	30–45	3–6	13–22	1.5–3	7.5–14
Tb	100–350	200–700	25–100	100–380	15–55	55–150
Dy	40–110	80–280	10–25	35–100	5–15	20–80
Ho	300–1400	620–3100	70–550	260–2200	40–300	155–850
Er	115–1200	230–3100	20–375	90–1500	15–200	90–575
Tm	1800–20000	3700–50,000	330–8000	1610–12,000	200–4000	940–10,000
Yb	400–5000	850–12,000	100–1500	350–4000	50–800	200–3900
Lu	2000–12000	4300–30,000	480–4800	1800–15,000	250–2500	1000–6500

[a] Composition of monazite minerals obtained from Manavalakurichi, Chavara, the Orissa Coast, and found in reference material IGS-36.

TABLE IV
Matrix Effects of Th, La, Ce, Pr, Nd, and Sm on HREE Determination

Matrix	Conc. ($\mu g\ mL^{-1}$)	HREEs Bias ($\mu g\ L^{-1}$)								
		Eu 387.967	Gd 342.247	Tb 350.917	Dy 353.170	Ho 345.600	Er 349.910	Tm 346.220	Yb 328.937	Lu 261.542
Th	500	2	58	1980	510	610	WOL	8	4	140
Th	1000	3	83	3840	990	1240	WOL	9	8	280
La	500		100	15	4		10	55		
La	1000		170	25	7	5	15	110		
Ce	500	WOL	2100	WOL	WOL	9	4	135	34	8
Ce	1000	WOL	4050	WOL	WOL	14	7	280	68	16
Pr	100	20	WOL	220	15	240	390	WOL	3	
Nd	500	1540	WOL	WOL	810	380	1890	75	WOL	
Nd	1000	3060	WOL	WOL	1580	740	3620	140	WOL	
Sm	100	WOL	80	2900	WOL	WOL	90			

Wavelength in nanometers. Blank indicates below detection limit. WOL = Wing overlap from matrix element.

and Lu). The results listed in Table IV indicate that in all cases either one or more elements present in major amounts caused serious interferences in the estimation of the HREEs; therefore, separation of the major portion of the interfering elements is required for the accurate determination of these elements.

Bis-(2-ethyl hexyl) hydrogen phosphate is used for the separation of individual REEs using the principle of counter-current chromatography (27). Hence, HDEHP was selected in this study to separate the LREEs from the HREEs. A systematic study was carried out on the extraction behavior of the REEs, Y, and Th by changing certain parameters, such as aqueous phase acidity, concentration of the extractant, and stripping agents.

Effect of HDEHP Concentration

The extraction of REEs depends on the concentration of the extracting reagent, aqueous phase acidity, and atomic number of the REEs. Solvent extraction studies with varying concentrations of HDEHP

(0.1M to 0.4M) from 0.1M HCl medium indicates that the extraction of HREEs from Eu to Lu was complete with 0.22M HDEHP in two-stage extractions.

Effect of Acid Concentration

A better separation factor is reported in chloride medium (27) rather than with nitrate and sulphate media; therefore, HCl was selected for detailed study. A moderate concentration of HDEHP (0.22M) was selected to study the effect of different HCl concentrations in the aqueous phase. The HCl concentration was varied from 0.05M to 0.2M. Using 0.1M HCl, the extraction of elements from Eu to Lu was complete in two extractions; however, the amount of co-extracted Nd and Sm was also greater, causing interference in the estimation of Eu. However, with 0.2M HCl medium, the co-extracted amount of Nd and Sm was considerably less, but the extraction of Eu and Gd was also incomplete (40% and 60%, respectively,) and others (Tb to Lu) were completed in two extractions. As a result, an acidity of 0.1M was fixed for the quantitative recovery of Eu and Gd, and 0.2M HCl was used for the remaining HREEs in two extractions. Since greater amounts of Nd and Sm (17% and 60%, respectively,) were associated with Eu and Gd, they were determined after applying dilution and interelement spectral interference corrections (26) for the partially extracted Nd on Eu. The extraction behavior observed in this study was similar to our earlier study on the separation of REEs from rock samples where we used a mixture of H_2MEHP and HDEHP (21).

On the basis of the above studies, the concentration of HDEHP was fixed at 0.22M. The elements Eu and Gd were extracted from 0.1M HCl medium, and the elements from Tb to Lu were extracted from 0.2M HCl medium.

Stripping of Rare Earth Elements

The chelation and co-ordination ability of REEs with HDEHP increases from La to Lu. Therefore, quantitative stripping of Tm, Yb, and Lu was very difficult even with 6M HCl. In our earlier study (21) of using a mixture of H2MEHP and HDEHP, we observed that addition of a small quantity of TBP enhances the stripping of HREEs, and if the concentration of TBP is more than 0.15M, quantitative stripping of all REEs could be achieved using a 4M HCl solution. However, in the present study and under the same conditions, a considerable amount of thorium (more than 70%) also accompanied the REE fraction. Since thorium is a potentially line-rich element, having either direct or wing overlaps on the majority of the HREE emission lines, removal of thorium from the aqueous strip is a must. We observed that the presence of H2MEHP in the organic layer would prevent the stripping of thorium. Hence, H2MEHP was added before the stripping stage. Due to the non-availability of pure H2MEHP, a mixture of HDEHP and H2MEHP was used. The concentration of H2MEHP was varied and it was found that at concentrations of 0.04M H2MEHP and above in the organic phase, the concentration of thorium found in the aqueous strip was less than 10 μg mL^{-1}, which is below the spectral interference level.

ICP-AES Determination of REEs and Y in Monazite Sample

The elements La, Ce, Pr, Nd, Sm, and Y, which are present at higher concentrations in the monazite mineral, were determined directly from the stock solution prepared after oxalate precipitation and after suitable dilution. A weak spectral interference of Nd on Pr was noticed and interelement interference correction (26) was applied. The presence of Ce up to 60 μg mL^{-1} did not cause any change in the net emission signal of 3 μg mL^{-1} Pr.

The aqueous strip (25 mL) containing Eu and Gd was diluted further to reduce the concentration of partially extracted Nd and Sm. The elements Tm and Lu were determined in the aqueous strip directly and Tb, Dy, Ho, Er, and Yb were determined after dilution (5– to 25-fold).

Accuracy and Precision

Table V lists the results of the ICP-AES determination of REEs and Y carried out on a monazite synthetic mixture (25 mg La, 50 mg Ce, 5.0 mg Pr, 25 mg Nd, 2.50 mg Sm, 50 μg Eu, 1500 μg Gd, 300 μg Tb, 1000 μg Dy, 100 μg Ho, 100 μg Er, 50 μg Tm, 100 μg Yb, 50 μg Lu, and 2500μg Y) by the proposed solvent extraction separation, indicating the quantitative recovery of HREEs. Table V also shows the results obtained on the monazite reference sample IGS-36 (28) and the syenite rock reference standard SY-3 (29). The SY-3 sample solution was prepared as reported earlier (21) and the extraction was carried out maintaining the required acidity. The data illustrate that the values obtained by the proposed method are in good agreement with the reported values. The %RSD (n=4) calculated for the monazite synthetic mixture and IGS-36 indicates good precision. Table VI lists the results of the REE and Y determination by the proposed method in three monazite minerals collected from Manavalakurichi, Chavara, and the Orissa coast. The concentration of Tm in these samples was below the determination limit. The recoveries of the HREEs were further verified by the standard addition method (doping known quantities of HREEs into the sample before the extraction). The recoveries obtained were complete

TABLE V
Comparison of REEs and Y Values in Synthetic Monazite Mixture, IGS-36 and SY-3, Obtained by the Proposed Method and the Reported Values

Elements	Synthetic Mixture			IGS-36			SY-3	
	Taken	Found	%RSD	Reported	Found	%RSD	Reported	Found
La	25.00	24.92	1.2	10.17	10.10	1.2	1340	1370
Ce	50.00	49.98	1.1	20.29	20.19	1.4	2230	2260
Pr	5.60	5.54	2.8	2.32	2.29	3.2	223	215
Nd	22.50	22.45	1.7	9.01	9.32	2.4	670	700
Sm	2.50	2.53	1.8	1.33	1.23	3.5	109	103
Eu	120	118	4.2	301	280	4.8	17	16.5
Gd	1.75	1.78	3.2	0.67	0.70	3.2	105	102
Tb	350	347	3.3	933	945	4.3	18	18
Dy	900	895	1.2	0.27	0.29	2.0	118	117
Ho	100	99	3.5	346	355	3.5	29.5	29.0
Er	125	123	4.1	535	607	4.0	68	70
Tm	40	39	6.0	57	64	6.3	11.6	12.0
Yb	70	68	2.8	295	350	3.7	62	63.5
Lu	25	24	4.8	51	46	3.8	7.9	7.6
Y	2.50	2.48	1.9	0.88	0.87	2.1	718	705

Synthetic mixture: Values of La, Ce, Pr, Nd, Gd, and Y are in mg, all other elements are in μg.
IGS-36: Values of La, Ce, Pr, Nd, Sm, Gd, Dy, and Y are in percentage, all other elements are in μg g^{-1}.
SY-3: All values are in μg g^{-1}.

TABLE VI
Results of ICP-AES Determination of REEs and Y in Monazite Minerals From Different Beach Sands of India

Element	Manavalakurichi		Orissa Coast		Chavara	
	Values	%RSD	Values	%RSD	Values	%RSD
La	15.80	1.3	17.20	1.2	18.88	1.0
Ce	39.22	1.0	39.55	1.1	38.52	1.2
Pr	4.85	3.2	4.68	3.5	4.46	3.0
Nd	19.52	1.8	17.60	1.9	17.38	2.2
Sm	2.80	3.6	2.61	3.7	2.50	3.4
Eu[a]	130	3.9	260	3.8	235	4.0
Gd	0.90	2.8	0.97	3.0	0.92	3.1
Tb[a]	530	3.7	660	4.0	590	4.2
Dy	0.15	1.6	0.21	1.5	0.18	1.8
Ho[a]	105	2.9	200	3.1	145	3.3
Er[a]	125	4.7	290	4.3	195	4.1
Tm[a]	<25	–	<25	–	<25	–
Yb[a]	47	3.1	56	3.2	55	3.1
Lu[a]	<10	–	10	4.3	10	4.1
Y	0.28	1.8	0.53	0.53	0.47	2.7

[a] Values are in μg g^{-1}; other elements are in percentage.

and the reproducibility is characterized by an RSD of 1–7%, depending on the concentration range.

CONCLUSION

Severe spectral interferences were observed in the ICP-AES determination of certain HREEs (Eu, Gd, Tb, Er, and Tm) in a monazite mineral matrix due to the presence of large quantities of La, Ce, Pr, Nd, and Th in the aspirated solution. The interfering elements were selectively removed using a combination of HDEHP solvent extraction from 0.1M and 0.2M HCl media, and stripping the extracted REEs in the presence of TBP and H2MEHP. Removal of the majority of La, Ce, Pr, Nd, and Th facilitates the accurate ICP-AES determination of Eu, Gd, Tb, Dy, Ho, Er, Tm, Yb, and Lu. The validity of the proposed method was verified by analyzing a synthetic monazite sample as well as geological reference materials IGS-36 and SY-3.

ACKNOWLEDGMENTS

The authors are thankful to Dr. H.C. Arora, Associate Director (Chemistry), AMD, Hyderabad; Shri V.P. Saxena, Regional Director, AMD, Central Region; Shri. P.K. Srivastava, In-Charge, Chemistry Lab; and Shri V.N. Dwivedi (Ex-In-Charge, Chemistry Lab), for their encouragement and for providing the necessary facilities. The authors are also thankful to the Director of AMD for granting the publication permission.

Received April 28, 2006.

REFERENCES

1. L.A. Haskin, “Rare Earth Elements in Geochemistry,” P. Henderson (ed.), Elsevier, Amsterdam, The Netherlands, pp. 115-148 (1984).
2. H. Elderfield and M.J. Greaves, Nature (London) 296, 214 (1982).
3. R.K. Malhotra, Proceedings of 10th ISAS National Symposium on Strategic and Hi-Tech Metals, Udaipur, India, IL-15, pg.1 (1994).
4. K.A. Gschneidner, Jr., and L. Eyring (eds.), Handbook of Physics and Chemistry of Rare Earths, Vol. 28, Elsevier, Amsterdam, The Netherlands (2000).
5. L.L.Y. Chang, R.A. Howie, and J. Zussman, "Rock-forming Minerals," Vol. 5B; Non-silicates and Halides, Longman Group Limited, England (1996).
6. Irena Jaron, Barbara Kudowska, and Ewa Bulska, At. Spectrosc. 21, 105 (2000).
7. R. Lara, R.A. Olsina, E. Marchevsky, J.A. Gasquez, and L.D. Martinez, At. Spectrosc. 21, 172 (2000).
8. R. Djigova and Ju. Ivanova, Talanta 57, 821 (2002).
9. M.R. Buchmeiser, R. Tessadri, G. Seeber and G.K. Bonn, Anal. Chem. 70, 2130 (1998).
10. M.I. Rucandio, Anal. Chim. Acta 264, 333 (1992).
11. N. Daskalova, S. Velichkov, N. Krasnobaeva, and P. Slavova, Spectrochim. Acta, 47(B), 1595 (1992).
12. S. Velichkov, N. Daskalova, and P. Slavova, Spectrochim. Acta, 48(B), E1743 (1993).
13. S. Velichkov, E. Kostadinova, and N. Daskalova, Spectrochim. Acta 53(B), 1863 (1998).
14. E. Kostadinova , L. Aleksieva, S. Velichkov, and N. Daskalova, Spectrochim. Acta 55(B), 689 (2000).
15. L. Aleksieva, E. N. Daskalova, and S. Velichkov, Spectrochim. Acta 57(B), 1339 (2002).
16. D.S.R. Murthy, B.K. Balaji, and S.P. Balakrishnan, At. Spectrosc. 11, 112 (1990).
17. K. Iwasaki and H. Haraguchi, Anal. Chim. Acta 208, 163 (1988).
18. J. Diffield and G.R. Gilmore, J. Radioanal. Chem. 48, 135 (1979).
19. J.G. Crock and F.E. Lichte, Anal. Chem. 54, 1329 (1982).
20. J.G. Crock, F.E. Lichte, G.O. Riddle, and C.L. Beach, Talanta 33, 601 (1986).
21. P.K. Srivastava and A. Premadas, J. Anal. At. Spectrom. 14, 1087 (1999).
22. A. Premadas and P.K. Srivastava , J. Radioanal. Nucl. Chem. 251, 233 (2002).
23. Z. Kplarik and H. Pankova, J. Inor. Nucl. Chem. 28, 2325 (1966).
24. G.W. Mason, D.N. Mehta, and D.F. Peppart, J. Inorg. Nucl. Chem. 38, 2077 (1976).
25. A.K. De, S.M. Khopkar, and R.A. Chalmers, "Solvent Extraction of Metals," Van Nostrand, New York, USA (1970).
26. Joachim Noelte, "ICP Emission Spectrometry A Practical Guide," Wiley-VCH Verlag GmbH & Co. KGaA, Weinheim, Germany, pg. 135 (2003).
27. J. Rydberg, C.Musikas, and G.R. Choppin, "Principles and Practices of Solvent Extraction," Marcel Dekker, Inc., New York, USA, pg. 398 (1992).
28. B. Lister, Geostand. Newsl. 2, 157 (1978).
29. K. Govindraju, Geostand. Newsl. (Special Issue), 18 (1994).